

We are IntechOpen, the world's leading publisher of Open Access books Built by scientists, for scientists

6,900

Open access books available

186,000

International authors and editors

200M

Downloads

Our authors are among the

154

Countries delivered to

TOP 1%

most cited scientists

12.2%

Contributors from top 500 universities



WEB OF SCIENCE™

Selection of our books indexed in the Book Citation Index
in Web of Science™ Core Collection (BKCI)

Interested in publishing with us?
Contact book.department@intechopen.com

Numbers displayed above are based on latest data collected.
For more information visit www.intechopen.com



Chapter

Use of Computed Tomography and Thermography for the Diagnosis of Respiratory Disorders in Adult Sheep

Luis Miguel Ferrer, Juan José Ramos, Enrique Castells, Héctor Ruíz, María Climent and Delia Lacasta

Abstract

Respiratory diseases are one of the main causes of death and economic losses in sheep farming. The prevention and treatment of these diseases must be based on a correct diagnosis, which improves the results of health plans and optimizes the responsible use of medicines. Diagnostic imaging techniques are important working tools to diagnose this kind of disorders but have not always been sufficiently used in sheep. X-ray, although widely used in small animals, is not a valuable tool in field conditions. Ultrasonography is a noninvasive technique easily applied in sheep farms and very useful for the diagnosis of respiratory diseases; however, many articles have been already published on this topic. The present paper proposes and illustrates the use of thermography and computed tomography (CT) to support and improve the aforementioned techniques, taking into consideration that thermography is only useful for upper respiratory tract disorders and CT scan is an expensive technique for routine use but very illustrative to understand the pathogenesis of the different disorders and to improve the in vivo diagnosis.

Keywords: thermography, computed tomography, sheep, respiratory diseases

1. Introduction

The respiratory system consists of a series of organs responsible for performing a set of physical and chemical processes that aim to absorb the air oxygen (O_2), essential for the oxidative phenomena that occur in the tissues, and the elimination of products resulting from these same oxidative phenomena, especially carbon dioxide (CO_2) [1]. The airways begin in the nares or external nasal openings and end at the level of the terminal bronchi, already within the lungs. These airways include an upper respiratory tract (nasal cavity, paranasal sinuses, nasopharynx, and larynx) and a lower respiratory tract (trachea and lung). This classification will be used to describe the respiratory disorders in this paper.

The development of effective health plans and the optimization of the use of drugs require an accurate diagnosis that assures that the treatment is addressed against the cause responsible for the pathological process. In this sense, diagnostic

imaging is a useful tool based on noninvasive techniques that provide images for the correct diagnosis of the different disorders. Although there are a wide variety of diagnostic imaging techniques appropriate for the diagnosis of respiratory disorders, this article focusses only on infrared thermography and computed tomography. Others such as radiography or ultrasound are not described here because there is an extensive series of published papers on these techniques.

Infrared thermography is an innovative noninvasive tool that allows the remote measurement of the surface temperature of an animal. A thermal imaging camera captures and records the measurement and creates a color thermal image, where each color corresponds to a specified temperature [2]. A computer program, associated with the camera, allows measuring the temperature of each point in the image and thus compares the different areas. There are different patterns of colors that can be chosen; in our case we will use the pattern that associates cold temperatures with blue, turning to green, yellow, orange, red, and white as the temperature of the area rises. Colors are not directly associated with the degrees of temperature; simply, the coldest area of the image is related to the blue color and the hottest area to the white color, whatever those temperatures are.

These properties make it especially useful for diagnosing upper respiratory tract diseases, where the internal temperature of the affected structures in the nasal cavities and sinuses comes to modify the surface temperature of the face. The generated image allows comparison of the left and right side of the animal, detecting which side is affected and if it produces changes in the ventilation of the nostrils. In winter, the cold air that the sheep breathes cools down the nostrils, and the diagnosis of the different disorders that hinder the passage of air is straightforward; however, with external high temperatures, closer to body temperature, it is more difficult to detect these changes. Nevertheless, the immediacy and the current low prices of the thermal cameras make the use of thermography suitable as one of the first tests to be carried out to diagnose upper respiratory tract diseases in sheep.

Computed tomography, also known as CT scanner, is also based on the variable absorption of X-rays by different tissues. However, CT provides a different form of imaging known as cross-sectional imaging. Therefore, this system provides images that are similar to anatomical sections of the structure of the animal studied. Different computer programs associated with the scanner allow obtaining axial, sagittal, and coronal sections. Also, it is possible to make color three-dimensional reconstructions of the studied area and to be able to introduce or remove different densities, which is equivalent to being able to observe different structures. In the case of the respiratory system, these programs allow us to eliminate all the structures and only leave the image of the surface of the airways, which is equivalent to having the negative image of the respiratory tree. Currently, CT scanner is only used with research purposes or for complex diagnosis in sheep; however, it is very valuable to understand the different respiratory diseases and their pathogenesis and evolution.

This article shows comparative images obtained by CT scan and thermography with those taken later at the necropsies of the animals. More than 80 respiratory clinical cases affecting adult sheep received at the Ruminant Clinical Service of the Veterinary Faculty of Zaragoza (SCRUM) have been studied using CT scan and thermography as imaging diagnostic tools. Subsequently, a *postmortem* examination was performed in all the cases. The final diagnosis was supported by histopathological, microbiological, and biomolecular analyses of the respiratory system of the studied animals.

To capture the images shown in this article, the used devices were the following:

- Thermographic camera: FLIR E63900, T198547. Images were performed at the Ruminant Clinical Service of the Veterinary Faculty of Zaragoza, Spain.

- Computed axial tomography: General Electric Healthcare. The CT scan model is: CT Brivo 325, General Electric. Images were performed at the Centro Clínico Veterinario of Zaragoza, Spain. The RadiAnt DICOM Viewer 4.6.9 program was used to analyze the images.

2. Respiratory tract disorders

2.1 Upper respiratory tract disorders

The upper airways provide an intricate space for filtration, tempering, and humidification of inspired air. There are a whole series of structures that can be affected by different pathological disorders. Dorsal, ventral, and medium turbinates and ethmoidal labyrinth are easily examined through thermography, this being of great relevance because there are several diseases that settle in these structures hindering or obstructing the passage of air.

Before starting with the description of the diseases that affect the upper respiratory tract, thermography and CT scan of these structures in a healthy animal will be shown. Therefore, the comparison between healthy and affected animals can be more easily understood.

In **Figure 1**, a zenith view of the head of a healthy sheep can be observed with air passing through the nostrils, cold in winter (**Figure 1a**) and warm in summer (**Figure 1b**). **Figure 2** shows a cross section of the head at the level of the second molar, where the internal structure of the ventral and dorsal turbinates can be seen both at necropsy (**Figure 2a**) and with tomographic images with and without an Airways filter (**Figure 2b** and **c**). In **Figure 3a** sagittal cut of the head avoiding the

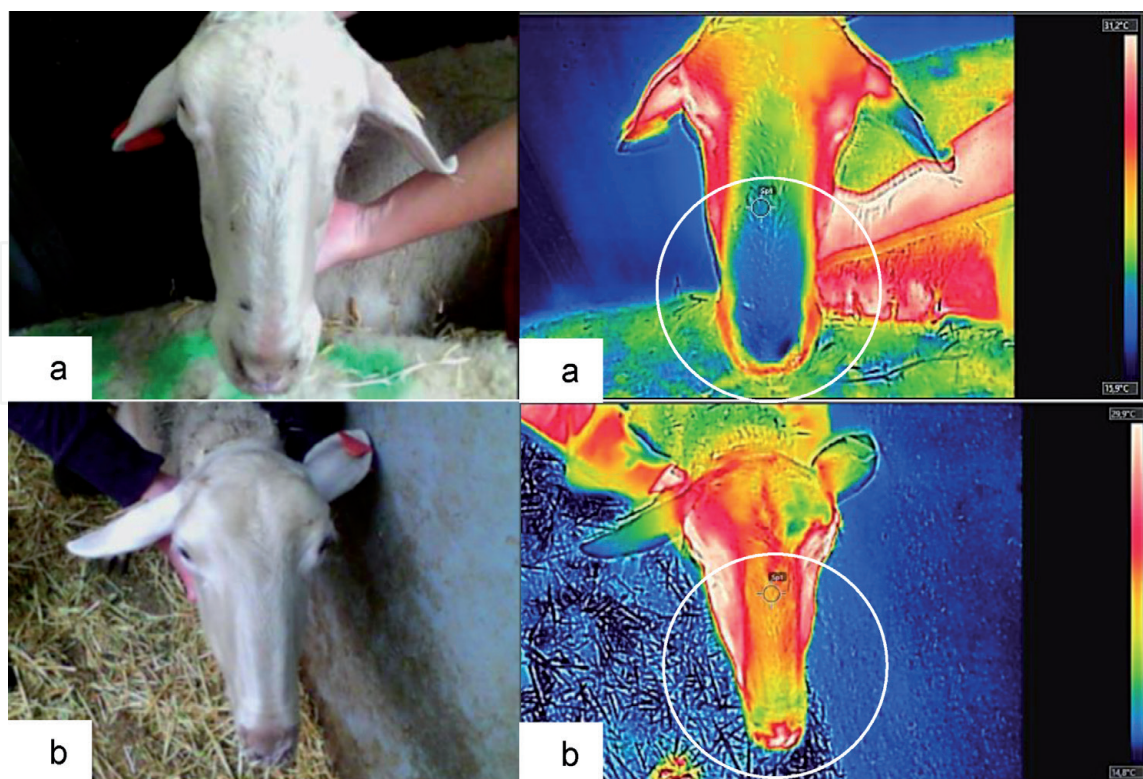


Figure 1. Zenith view of the head of a healthy ewe. (a) Picture of the ewe's head and its thermographic image with symmetrical cooling of the nostrils with cold external temperature (cold colors = blue and green). (b) Ewe's head picture and its thermography with symmetrical cooling of the nostrils with warm external temperature (warm colors = yellow and light green).

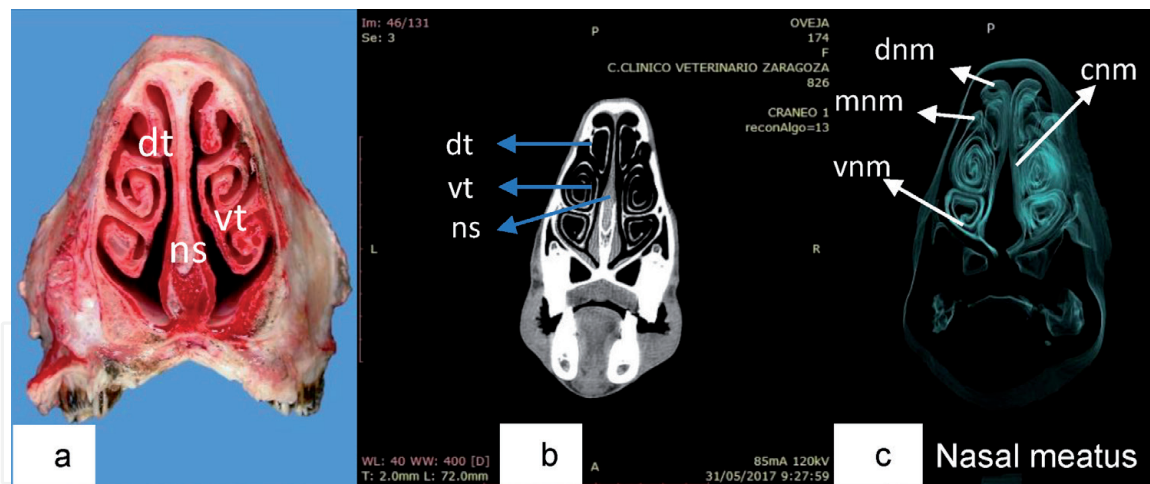


Figure 2. Nasal cavity of a healthy ewe. (a) Axial section of the head at the level of the second molar (dt dorsal turbinate, vt ventral turbinate, ns nasal septum). (b) CT axial view at maxillary sinus level (dt dorsal turbinate, vt ventral turbinate, ns nasal septum). (c) CT axial 3D view with airways filter. Surfaces view delimiting the air ducts or nasal meatus (cnm—common nasal meatus, dnm—dorsal nasal meatus, mnm—medium nasal meatus, vnm—ventral nasal meatus).

nasal septum with the structures of all turbinates can be seen (**Figure 3a–c**). The spatial placement of the different airways within the bone structure of the skull is appreciated.

Paranasal sinuses (maxillary, frontal, and lacrimal) and nasal septum have less diagnostic importance due to their low frequency of injury. **Figure 4** shows an axial section of the head at the level of the ethmoidal turbinate where the lacrimal paranasal sinuses can be seen (**Figure 4a and b**). Sporadically, alterations of the pharynx and larynx are diagnosed.

Below we will explain the different disorders that affect the upper respiratory tract in sheep and how imaging techniques can help in their diagnosis.

2.1.1 Chronic proliferative rhinitis

Chronic proliferative rhinitis (CPR) is an upper respiratory tract disease of sheep associated with *Salmonella enterica subsp. diarizonae* serovar 61:k:1,5,(7) (SED) which was described for the first time in the United States in 1992 [3] and, subsequently, in Spain [4, 5], again in the United States [6] and Switzerland [7]. In addition, it has also been diagnosed in the United Kingdom and Brazil (personal communications).

SED is a saprophytic microorganism in sheep; however, when this bacterium becomes intracellular, it produces an intense inflammatory reaction in the ventral turbinate, giving rise to the classical clinical signs of the disease [5]. This fatal prognosis disease causes loss of weight, no fever, snoring, seromucous nasal secretion, and nasal deformation. It can be unilateral or bilateral and regional lymph nodes are usually enlarged. Over time, these signs get worse, and, sometimes, it is possible to see inflammatory proliferative tissue at the nares [4, 5, 7]. Further, the inadequate flow of air in affected animals provides a better situation for opportunistic bacteria that lead to secondary pulmonary diseases that usually are responsible for the final death of the animals [5].

At *postmortem* examination, the ventral turbinates are presented swollen with a roughened surface (**Figure 5a**). The section of the turbinate shows a proliferative tissue that is usually composed of multiple small white or yellow polypoid structures covered by mucus, although, sometimes, only a thickening of the mucosa

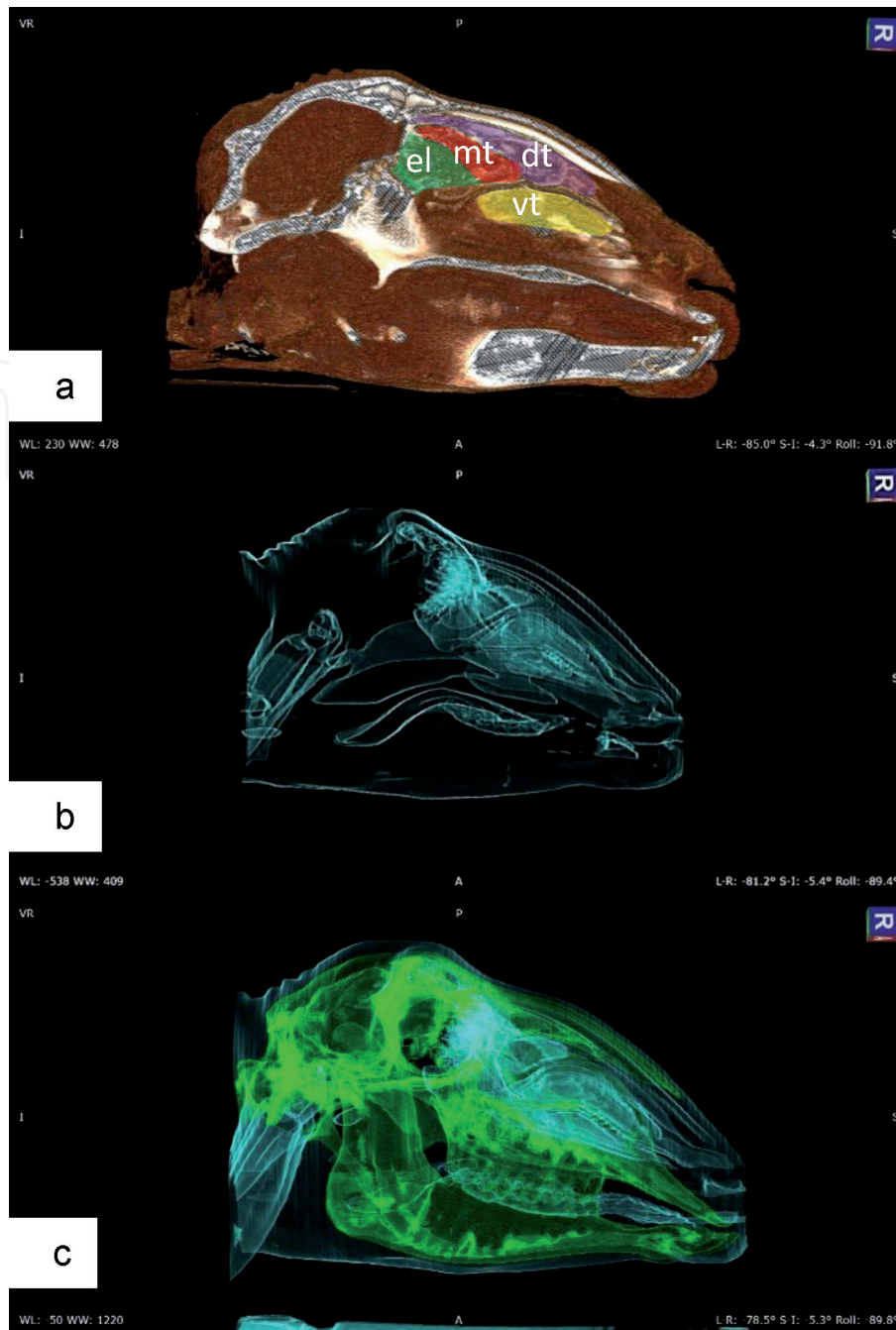


Figure 3. CT 3D sagittal views of a healthy ewe. (a) Sagittal cut of the head avoiding the nasal septum. The structures of all turbinates (dt dorsal turbinate, mt medium turbinate, vt ventral turbinate, and el ethmoidal labyrinth) are highlighted. (b) The same cut as 3a with airways filter to show the areas with air (blue). (c) Sagittal section with filter for airways (blue) and bone (green). The spatial placement of the different airways within the bone structure of the skull is appreciated.

can be observed [4]. Occasionally, the dorsal and medium turbinates may also be affected [8].

Thermographic images of CPR cases detect high temperatures (white and red colors) in the nostril area corresponding to the swollen ventral turbinate, and the difficulty of ventilation of the nasal cavity can also be observed (Figure 5b).

Computed tomography enables to obtain a clear image of the damaged tissue and the different stages of development of the disease (Figure 6). It also shows the increase in size of swollen turbinates and the bone destruction in more advanced cases. Axial slides show uni- or bilateral lesions, while sagittal slides detect affected turbinates, generally the ventral and less frequently the dorsal (Figure 6a–d).

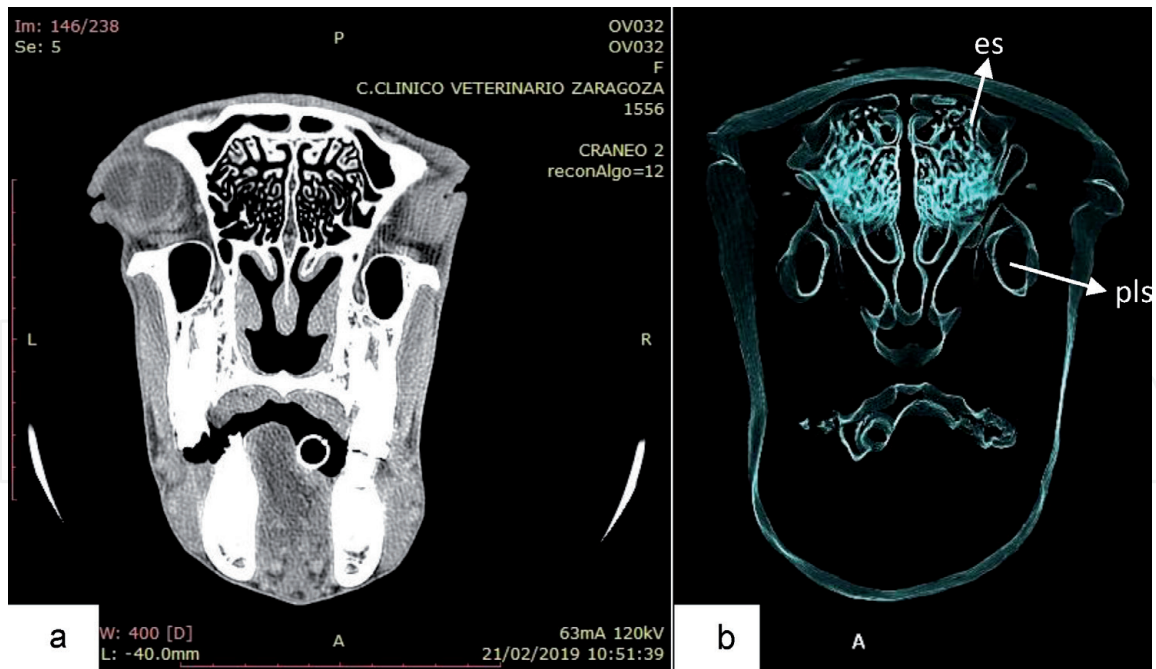


Figure 4. Ethmoidal turbinate of a healthy ewe. (a) CT axial view of the head at ethmoidal turbinate level. (b) CT axial 3D view with airways filter. View of the aerial surfaces of the ethmoidal sinuses (es) and the paranasal lacrimal sinus (pls).

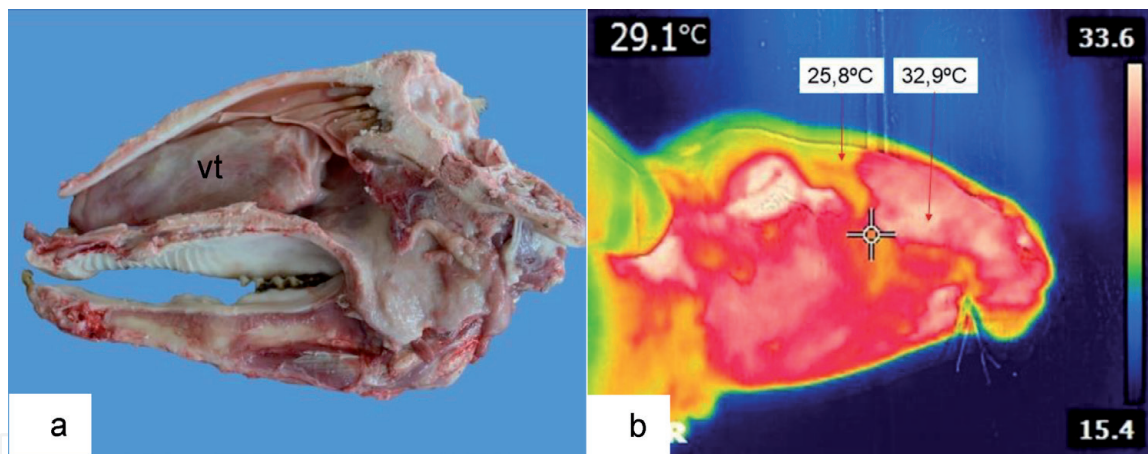


Figure 5. Chronic proliferative rhinitis. (a) Sagittal cut of the head avoiding nasal septum. Enlarged ventral turbinate (vt) is appreciated. (b) Thermography of the right side of a CPR-affected sheep with a relevant increase in temperature in the swollen area.

2.1.2 Enzootic nasal adenocarcinoma

Enzootic nasal adenocarcinoma (ENA) is a contagious tumor of the ethmoid turbinate mucosa caused by a betaretrovirus known as enzootic nasal tumor virus 1 (ENTV-1), which only affects sheep [9]. Goats can also be affected by an enzootic nasal adenocarcinoma which is caused by an enzootic nasal tumor virus of goats (ENTV-2) [9, 10]. It is a contagious chronic disease of the upper airways that has been described in farms all over the world, except in New Zealand and Australia [9].

ENA prevalence in the affected flock is variable, ranging from 0.1 to 15% [9]. Preferentially, the virus affects young adults, and several cases are usually observed in the same flock. No genetic, breed, or sex predisposition has been observed [9, 11–13].

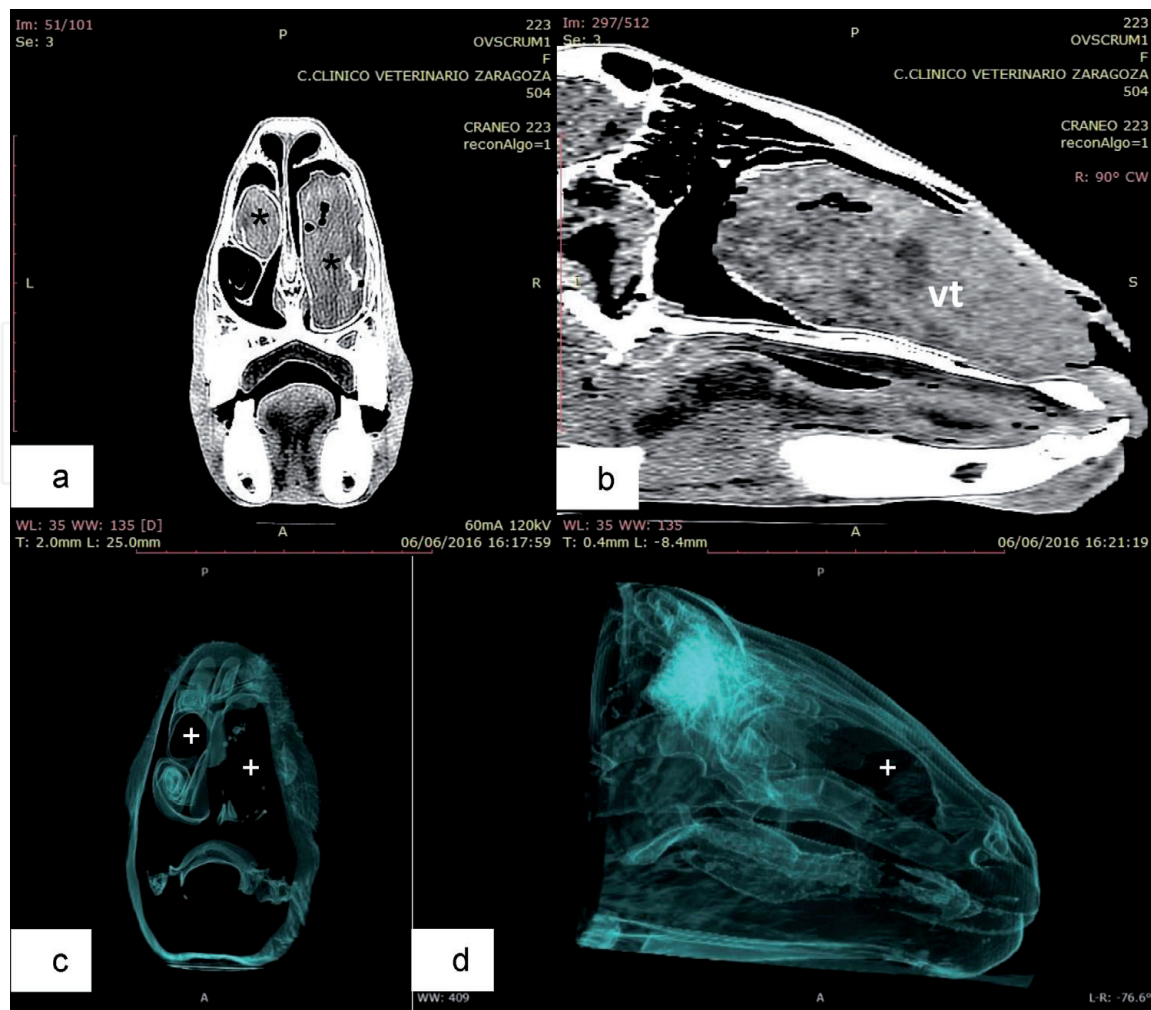


Figure 6.

Chronic proliferative rhinitis. (a) CT axial view of the head with bilateral CPR, predominantly on the right side. Gray masses () are the swollen turbinates. (b) CT sagittal view of the head in right nasal turbinate. Ventral turbinate (vt) increased in size is appreciated. (c) CT axial 3D view with airways filter. Black spaces of the nasal cavity (+) are swollen, airless masses. (d) CT sagittal 3D view with airways filter. The large black surface (+) represents the swollen mass of CPR.*

The most recognizable clinical sign of ENA is the unilateral serous nasal discharge that leads to a “washed nose” appearance, which is caused by the depilation of the area due to the continuous discharge. In advanced cases, the disease shows characteristic clinical signs such as snoring, coughing, and head shaking together with exophthalmos and softening and deformation of the skull bones (mainly frontal and maxillary) that can lead to the presentation of a skin fistula. Body condition is gradually lost, and animals eventually die due to bacterial complication of the tumor which ends with pneumonia or septicemia [9].

At necropsy, tumors are found in the nasal cavity arising from the ethmoidal mucosa and effacing the normal architecture of the ethmoidal conchae. Tumors are soft, gray, or reddish-white in color with a fine granular surface and covered with mucus (**Figure 7a**).

In ENA cases, the thermography shows reddish or even white colors in the posterior segment of the nose, matching the hottest areas (white color) with the ethmoidal bone, where the ENA is located (**Figure 7b**). The nasal cavity presents also a red color because, due to the obstruction provoked by the tumor, air cooling the area cannot pass through the nose. In the case of fistulizing and pouring liquid through the hole, the wet area can present colder tones (green, yellow) due to the evaporation of this liquid.

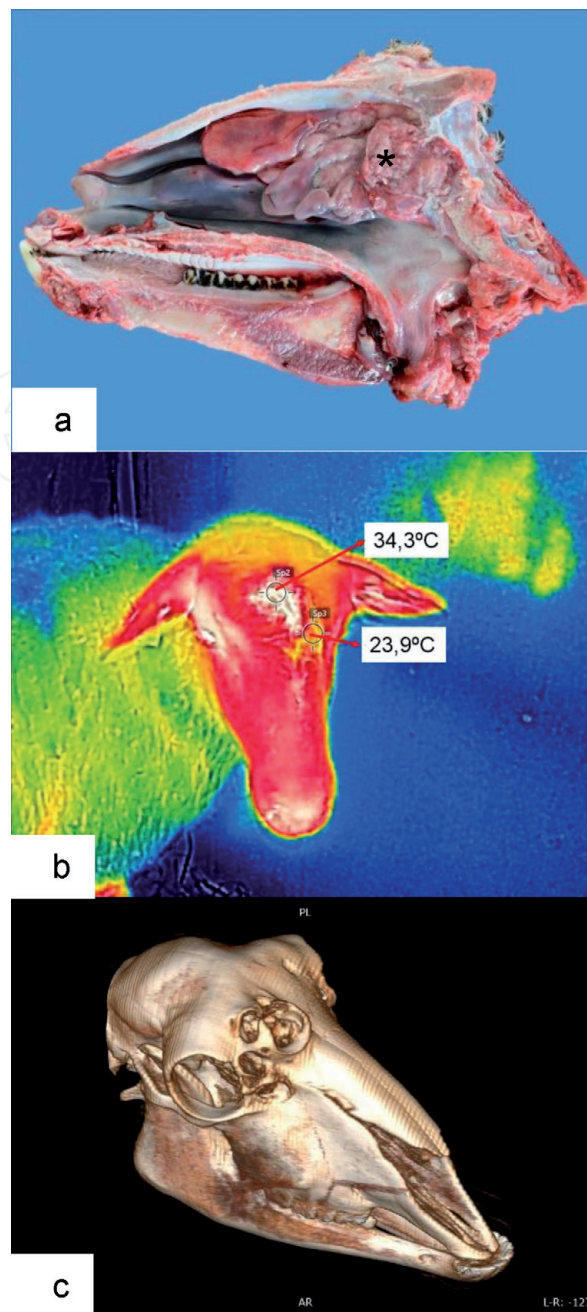


Figure 7. Enzootic nasal adenocarcinoma (ENA). (a) Postmortem findings of ENA with polyps (*) affecting the ethmoidal turbinate. (b) Thermography. Warmer area in the right side that matches the location of the tumor. (c) CT 3D view with soft tissue removal: skull with ENA and great bone rarefaction. The lithic process causing some holes in the nasal and lacrimal bones is shown.

The CT scan of ENA cases shows the destruction of the ethmoidal bone, the lithic curse of the nasal bone, and the soft tissues growing, sometimes with polyps in the distal part of the lesion (**Figure 8**), even before the nasal bone is destroyed and the face deformed (**Figure 7c**).

2.1.3 Oestrosis

Oestrosis is a worldwide cavitory myiasis caused by the larvae of the fly *Oestrus ovis* (Linnaeus 1761, Diptera, Oestridae) that develops from the first- to the third-stage larvae, which are obligate parasites of the nasal and sinus cavities of sheep and goats [14, 15]. In areas with semiarid climatic conditions, as in the Mediterranean countries, oestrosis is the most important upper respiratory tract disease from a clinical and economic point of view [16].

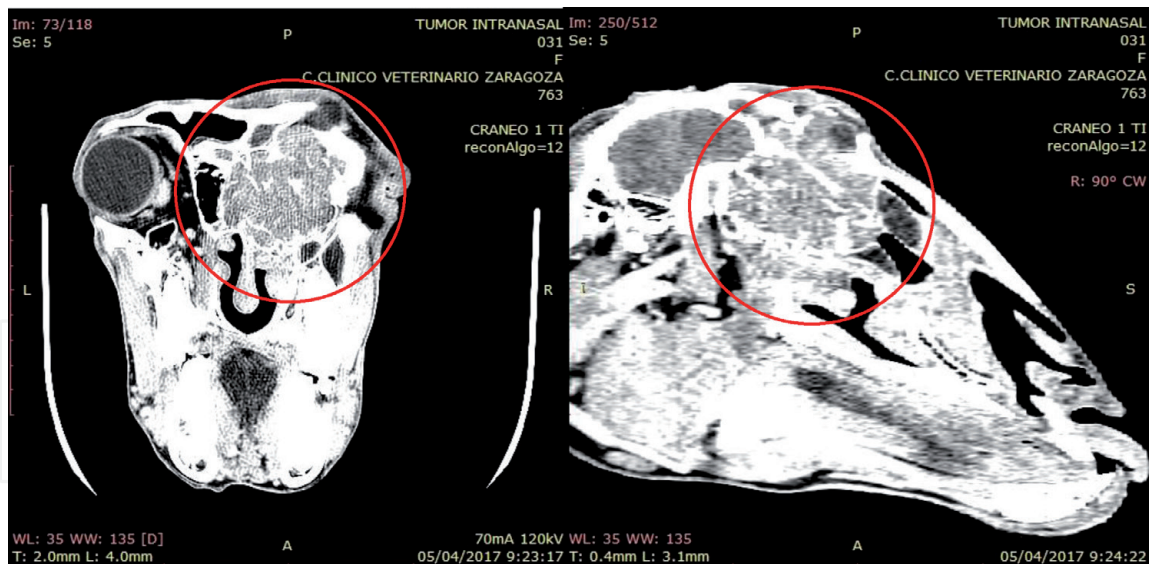


Figure 8.
Enzootic nasal adenocarcinoma. CT axial and sagittal view of an ENA in the right side of the skull (red circles).

Oestrosis is a collective disease with a high prevalence in which clinical signs have a seasonal variation, being more severe during hot and dry periods [15, 17]. The larvae produce chronic inflammatory rhinitis, and the affected animals present mucus, purulent, or even hemorrhagic nasal discharge [16, 18, 19]. Inspiratory dyspnea, frequent sneezing, head shaking, and emaciation are clinical signs that often accompany the mucopurulent nasal discharge [14, 15].

For the diagnosis of this disease, thermal images are not used unless the parasitization is very severe. CT images are only useful in the final stage of the larvae (L3). Tomographic pictures show the secretions, the swollen tissues of the turbinates, and even the segments of the larvae (**Figure 9a–c**), but its clinical use is not justified in this disease.

2.1.4 Intranasal abscess

As in other body areas, bacterial abscesses can be found inside the nasal cavity, causing distress and respiratory disorders [20–22]. These abscesses can even lead to facial deformation and fistulization (**Figure 10a**).

In thermographic images high temperatures (red and white colors) can be observed on the affected area (**Figure 10b**). Although the thermal camera will only provide useful images if the abscess is attached to the surface or if bone rarefaction has occurred. Nevertheless, CT delivers valuable images of abscess location, size, and content; likewise, the damage to the different surrounding tissues and the invasion to the nearby areas can be observed (**Figure 11**).

2.1.5 Sinusitis

Generally, primary sinusitis is caused by an upper respiratory tract infection of the paranasal sinuses, and secondary sinusitis is caused by a tooth root infection [23]; however, frontal sinusitis can be caused by an upper respiratory tract infection or by the breaking of a horn or an inappropriate dehorning [24, 25].

There is a close relationship of the maxillary posterior teeth to the maxillary sinus, so a periapical dental infection or the breaking of a tooth can cause a secondary infection of this sinus [26]. Also, inflammation and swelling in the nasal mucosa

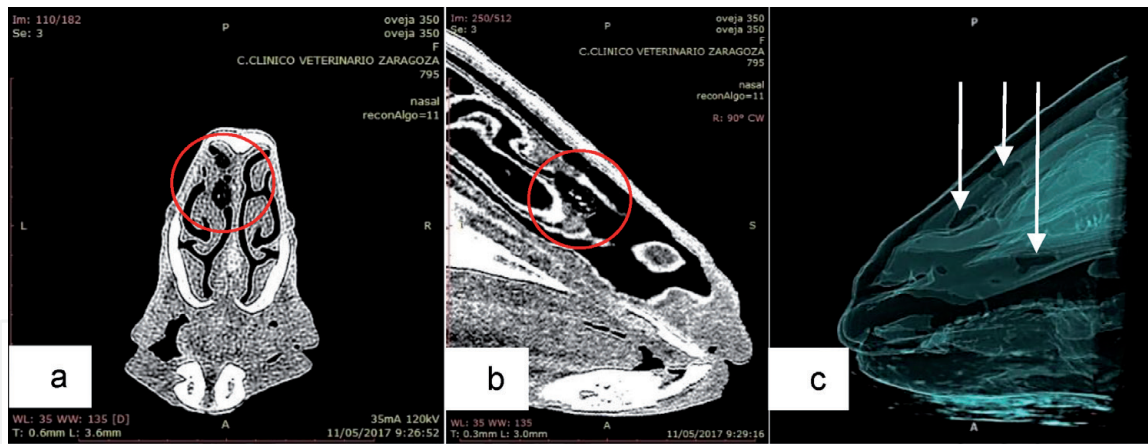


Figure 9. Oestrosis. (a) CT axial view of a sheep head affected by oestrosis. A larva cut crosswise between the ventral and dorsal turbinate is shown. Another small larva in the dorsal turbinate and mucus in the common nasal meatus is appreciated (red circle). (b) CT sagittal view with the presence of a crosswise cut larva in the cranial area of the ventral turbinate (red circle). (c) CT 3D view with airways filter. This technique shows the larvae-occupied areas and the mucus as black airless areas (white arrows).

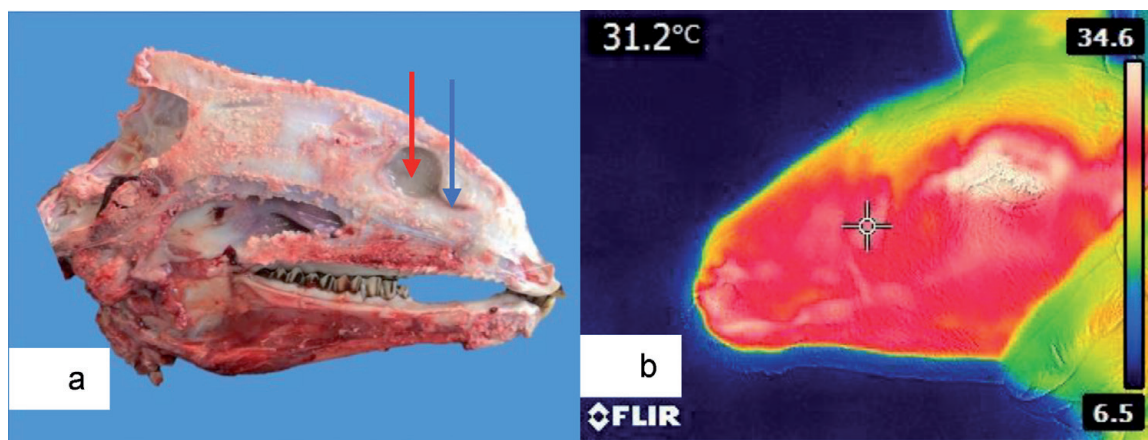


Figure 10. Intranasal abscess. (a) Postmortem findings of a circular abscess in nasal septum (red arrow) with a fistula draining into the common nasal meatus (blue arrow) are shown. (b) Thermography. A warmer area (whiter crossed zone) is seen in the projection of the abscess than in the surrounding tissues.

from a viral or bacterial infection could obstruct the nasomaxillary opening, blocking sinus drainage and predisposing to a sinusitis [23].

In sheep, there are a huge range of possible etiologies that can cause sinusitis: mycosis, such as those produced by *Conidiobolus* sp., as it has been described in sheep in Brazil and Uruguay causing necrotic sinusitis [27]; or due to the action of *Oestrus ovis* larvae [15, 28]; or by a wide variety of bacterial agents [23, 29].

The thermographic camera captures the focal heat that reaches the outside (Figure 12), since the sinuses are close to the surface of the animal's face. Using CT scan, the modification of the different structures, dental problems, or horn disorders can be studied (Figure 13).

2.1.6 Pharynx abscesses

The respiratory processes of the pharynx and larynx are scarcely diagnosed in sheep. Cases of pharyngeal abscess [22] or sarcocystis infestation in the larynx, causing laryngeal hemiplegia [30], have been reported but always as individual cases of very low prevalence. Further, laryngeal chondritis has been widely described in Texel and Southdown breeds in the UK and leads to breathing

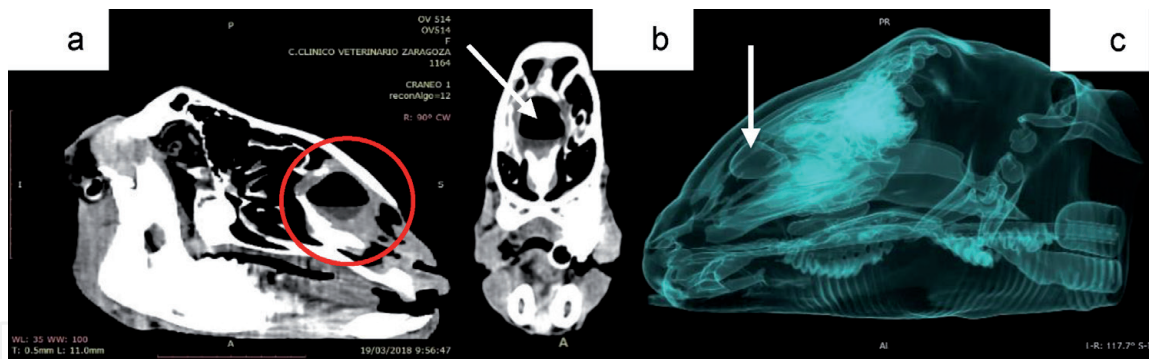


Figure 11. Intranasal abscess. (a) CT sagittal 3D view of a head with an intranasal abscess located in the nasal septum. An abscess full of air in the upper area and pus in the lower area is shown (red circle). (b) CT axial view of the same abscess (white arrow). (c) CT 3D view with airways filter. This technique shows a flat-bottomed bubble generated by emptying the part of the pus from the abscess through the fistula (white arrow).

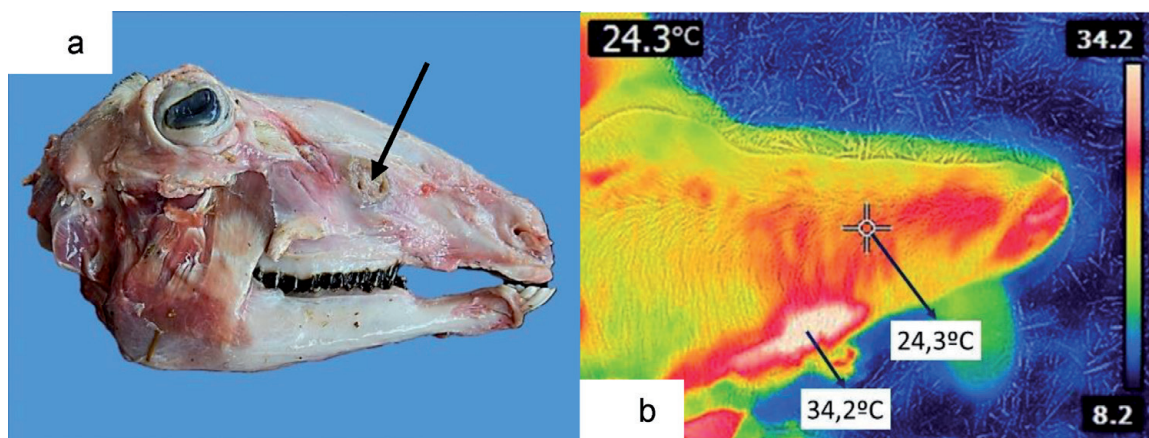


Figure 12. Maxillary sinusitis. (a) Bone rarefaction without fistulization (black arrow). (b) Thermography. Warmer area (white) compared to a normal point in the center of the image (white cross).

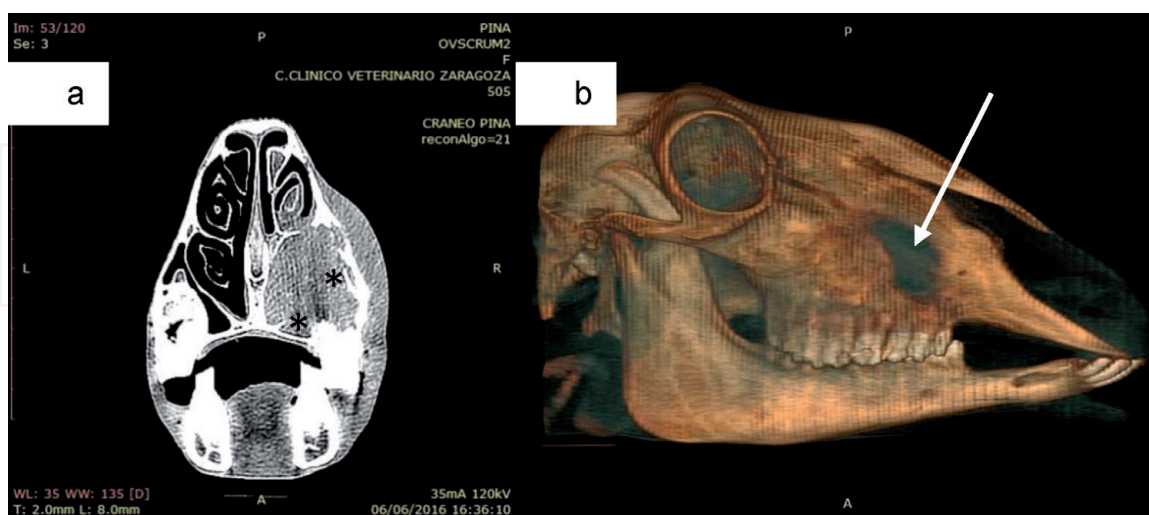


Figure 13. Maxillary sinusitis. (a) CT axial view with purulent material accumulation in palatine and maxillary sinus (*) which causes ventral turbinate and face deformation. No tooth pathology was found. (b) CT 3D view. Bone rarefaction without fistulization (white arrow).

problems, with swelling and discharges in the larynx [31], but it has never been diagnosed in Spanish breeds.

Caseous lymphadenitis (CLA) is a common disease in sheep affecting lymph nodes. If *Corynebacterium pseudotuberculosis*, the etiological agent, infects the

retropharyngeal or submandibular lymph nodes, these can press the pharynx and larynx producing deformation and respiratory distress [22].

Thermographic and tomographic images will not have a fixed pattern, depending on the affected structures. CT images contribute to clarify how the abscess is and in what structure the pressure causing respiratory distress is being produced (**Figure 14**).

2.2 Lower respiratory tract disorders

The trachea is a non-collapsible and about 25 cm long tube formed by incomplete 48–60 cartilaginous rings in the sheep and the goat (**Figure 15**). In sheep, the cross-sectional outline of the trachea differs from one region to another. In the larynx region, the outline is round, but with a low dorsal crest, whereas the middle-third of the trachea is U-shaped, as in the goat.

The lungs are the respiratory organs responsible for performing several functions; the gas exchange is the most important. They are also accountable for the elimination of foreign bodies carried by air through the mucociliary clearance and alveolar macrophages, and finally, the lungs also perform metabolic and endocrine functions, activating the inactive prohormones or protecting the organism from potentially toxic vasoactive substances [32]. Each lung occupies a pleural cavity (pleural sacs), and between them lays the mediastinum, a complex area that divides

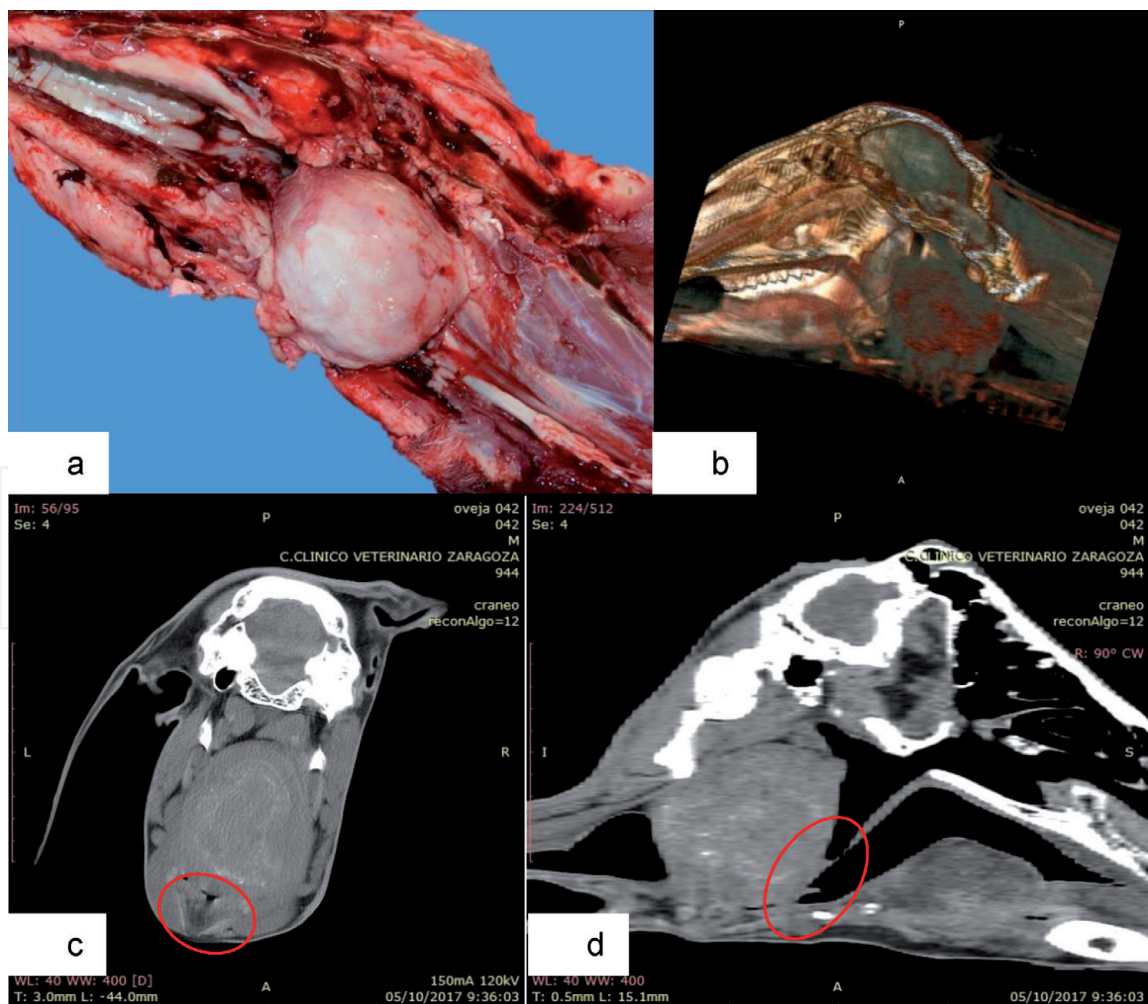


Figure 14. Eight centimeter diameter larynx abscess caused by *Corynebacterium pseudotuberculosis*. (a) Postmortem findings show a large abscess in pharyngeal area. (b) CT 3D view. Spatial location of the abscess in relation to pharynx and larynx. (c) CT axial view. Compression of larynx cartilage (red circle). (d) CT sagittal view. Pressure on the larynx and contact with the veil of the palate (red circle).

the thorax into two symmetrical halves [33]. In sheep, respiratory diseases are the main described disorders, producing high morbidity and mortality [34].

In a healthy sheep, the lungs take the shape of a half cone, with an apex at the upper part and an oblique base applied against the diaphragm (diaphragmatic face) (**Figure 16a**). Their lobulation does not exactly coincide with the large appreciable fissures in the pulmonary surface and follows the division of the trachea in the lobular bronchi. Both lungs have a cranial lobe (apical) and a caudal lobe (diaphragmatic), respectively, ventilated by a cranial and caudal bronchus. In addition, the right lung has a middle lobe and an accessory lobe, ventilated each with its corresponding bronchus. The right cranial bronchus in ruminants rises directly from the trachea, and the accessory lobe is mainly attached to the middle lobe rather than to the caudal lobe as in other mammals [35]. Dorsal and ventral CT 3D images with Airways filter and dorsal and ventral view of a silicon mold of the lung are shown in **Figure 16b–e**.

The main lower respiratory tract disorders will be detailed here below taking into account the tomographic support in its diagnosis.

2.2.1 Tracheal crushing

In intensive and semi-intensive production systems, tracheal crushing (**Figure 17a**) is a common disorder [35]. It seems clearly influenced by age, and recent surveys associate these lesions with management patterns when feeding animals. It is supposed that the type of feeders used during the periods of confinement can result in a key point to avoid this injury [35]. Some works relate this disorder to a worsening of animal welfare [36]. In addition, it has also been observed that these animals that presented tracheal crushing had a greater predisposition to suffer lower respiratory tract diseases [37].

CT images allow assessing the lumen of the trachea and locating the injured tracheal rings, visualizing the internal surface of this airway (**Figure 17b–d**).

2.2.2 Verminous pneumonia

Verminous pneumonia is caused by the mechanical and irritant action of parasitic nematodes, belonging to the order of Strongylida. Sheep is host to several lungworm nematode species of the families Dictyocaulidae (Trichostrongyloidea)

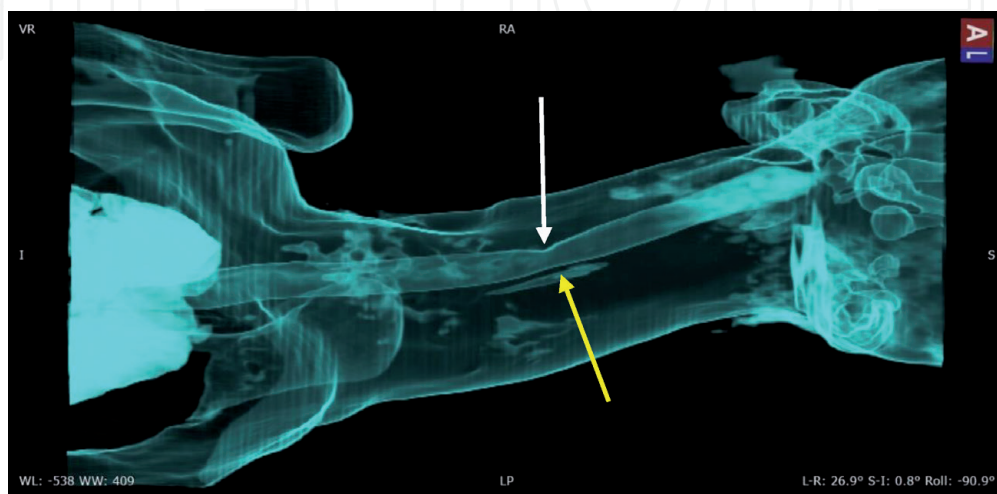


Figure 15. CT 3D view with airways filter. Trachea of a healthy animal with a depression caused by a tracheotomy (white arrow) performed a few hours before the CT scan and a small trace of extravasated air (yellow arrow).

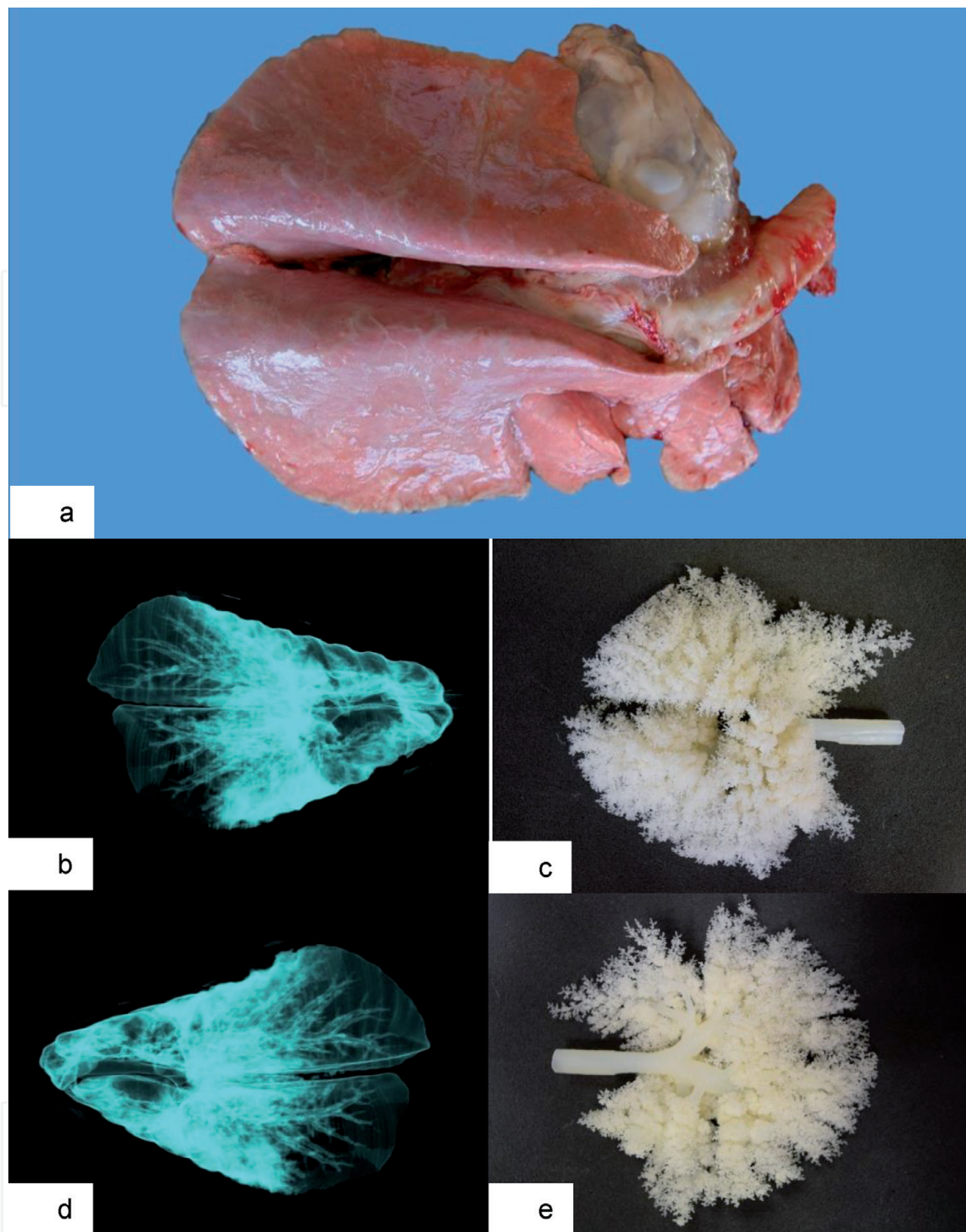


Figure 16. (a) Healthy lung. (b and d) Dorsal and ventral CT 3D images with airways filter. (c and e) Dorsal and ventral view of a silicon mold of the lung.

and Protostrongylidae (Metastrongyloidea) that induce verminous pneumonia, also called dictyocaulosis and protostrongylidosis. *Dictyocaulus filaria*, a thin white trichostrongylid-like nematode up to 10 cm long, is the largest sheep lungworm and affects caudal and diaphragmatic lung lobes. The most common protostrongylid species found in sheep are *Muellerius capillaris*, *Protostrongylus rufescens*, *Protostrongylus brevispiculum*, *Cystocaulus ocreatus*, and *Neostrongylus linearis* [38], which produce nodular pneumonic areas in the dorsal part of the lung.

Although, in endemic areas, lambs may show cough and unthriftiness during the first grazing season, in adults, clinical signs of pneumonia or other respiratory symptoms have rarely been observed, being pathological findings identified only

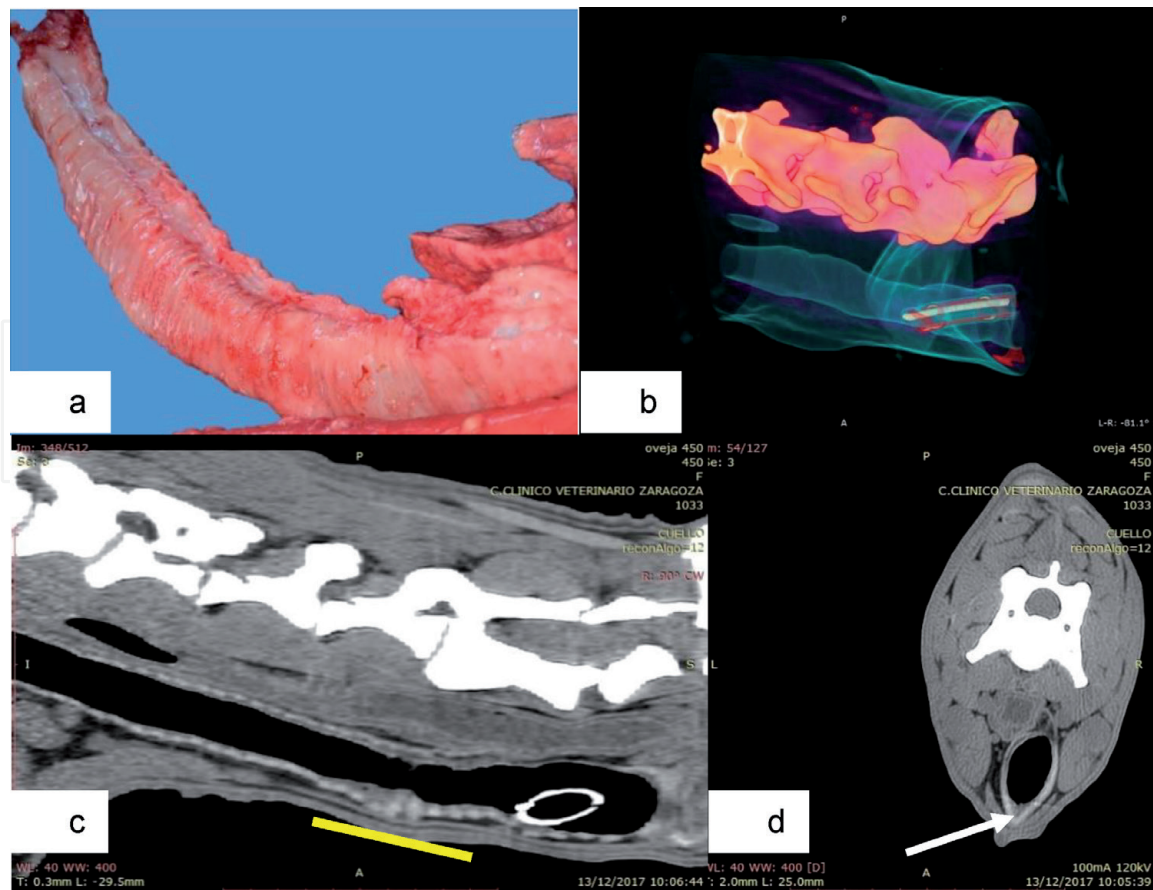


Figure 17. Tracheal crushing. (a) Necropsy shows the trachea with different flattened rings. (b) CT 3D view with bones and skin 3 filter. Tracheal lumen view with obvious deformations. (c) CT sagittal view. Severe deformation of tracheal rings (yellow line area). (d) CT axial view. Crushed tracheal ring with deformation in ventral area (white arrow).

at necropsy. Thus, two different types of subpleural nodules can be found: the verminous nodules containing a single worm that may be calcified and the breeding nodules, ranging from less than 1 mm to several centimeters in diameter, non-calcified, and containing mature reproducing adults and larvae. These nodules can be macroscopically observed as hard, slightly prominent, and greenish-gray due to the infiltration of eosinophils [39] (Figure 18a).

In the case of dictyocaulosis, computed tomography images show an increased thickness of the caudal and diaphragmatic areas of the lung, whereas in protostrongylidosis, nodular pneumonic areas located in the dorsal part of the lung can be observed (Figure 18b–d).

2.2.3 Lung abscesses

The lungs are continuously exposed to air that contains dust, bacteria, fungi, viruses, and various noxious agents [40, 41], favoring the development of different diseases, including abscesses. These abscesses are often caused following previous lung damage, secondary to other lung injuries, or may follow an embolic spread from another focus of infection [42].

Abscess is a necrotizing lesion characterized by a pus-filled cavity that is encapsulated by fibrous tissue [43] that can be located anywhere in the lung, such as pleura and lung parenchyma (Figure 19a), or even in regional lymph nodes, as mediastinal lymph nodes.

There are a great variety of bacteria that can cause lung abscesses, such as *Corynebacterium pseudotuberculosis*, *Trueperella pyogenes*, *Staphylococcus aureus*,

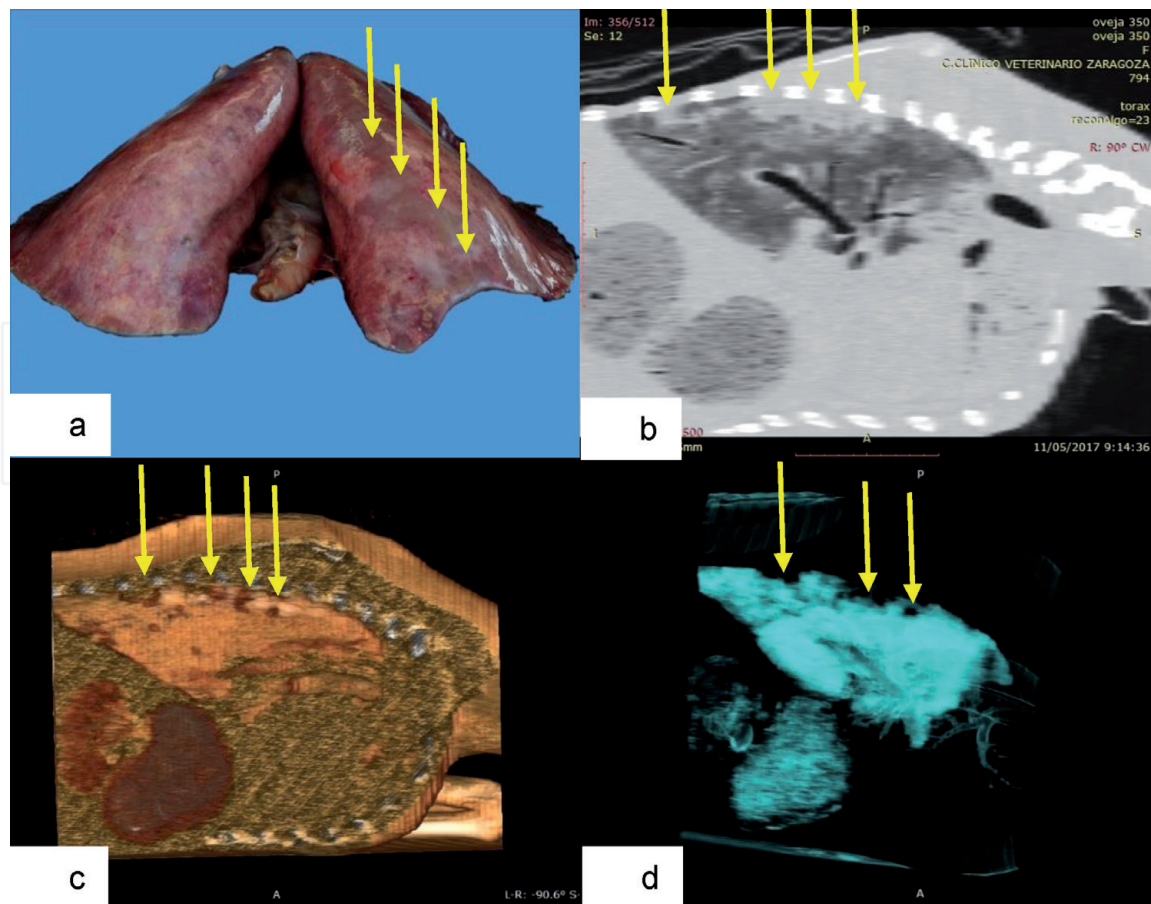


Figure 18.

Verminous pneumonia. (a) Pathological findings of a lung affected with verminous pneumonia, especially appreciated on the right side (yellow arrows). (b) CT sagittal view of the right lung with higher density whitish nodules in the dorsal area (yellow arrows). (c) CT 3D sagittal view of the right lung. The gaps in the dorsal area correspond to the consolidated areas of the lung (yellow arrows). (d) CT 3D sagittal view with airways filter. Black areas (yellow arrows) show the location of the nodules.

Fusobacterium necrophorum, *Mycobacterium tuberculosis*, *Streptococcus pyogenes*, *Escherichia coli*, etc. [40, 44, 45].

Computed tomography provides a specific image of the abscesses, their location (**Figure 19b** and **c**), and injured tissues involved in the disease (**Figure 19d**) as well as non-air flow pulmonary parenchyma. Frequently, an enhanced area around the abscess and mineralization within the abscess due to caseous necrosis, especially in the case of *C. pseudotuberculosis* infection, can be observed.

2.2.4 Ovine respiratory complex in adults

As ovine respiratory complex (ORC) in lambs, in adults, ORC is a complex disease involving a range of host-pathogen-environment interactions, where host immunological and physiological mechanisms interact with multiple etiological agents including bacteria, plus environmental factors or stressors [46]. There are three clinical presentation forms of the disease: hyperacute or peracute, characterized by sudden deaths due to septicemia; acute and subacute forms, with the classical clinical signs of a pneumonic process, whose severity will vary depending on the degree of lung consolidation; and chronic pneumonia with mild or unapparent clinical signs and fibrous tissue increasing the severity of consolidation [46].

Several infectious agents have been associated with ORC: *Mannheimia haemolytica*, *Pasteurella multocida*, *Bibersteinia trehalosi*, and *Mycoplasma* sp., which usually are found mixed in the isolates with more than one bacteria species

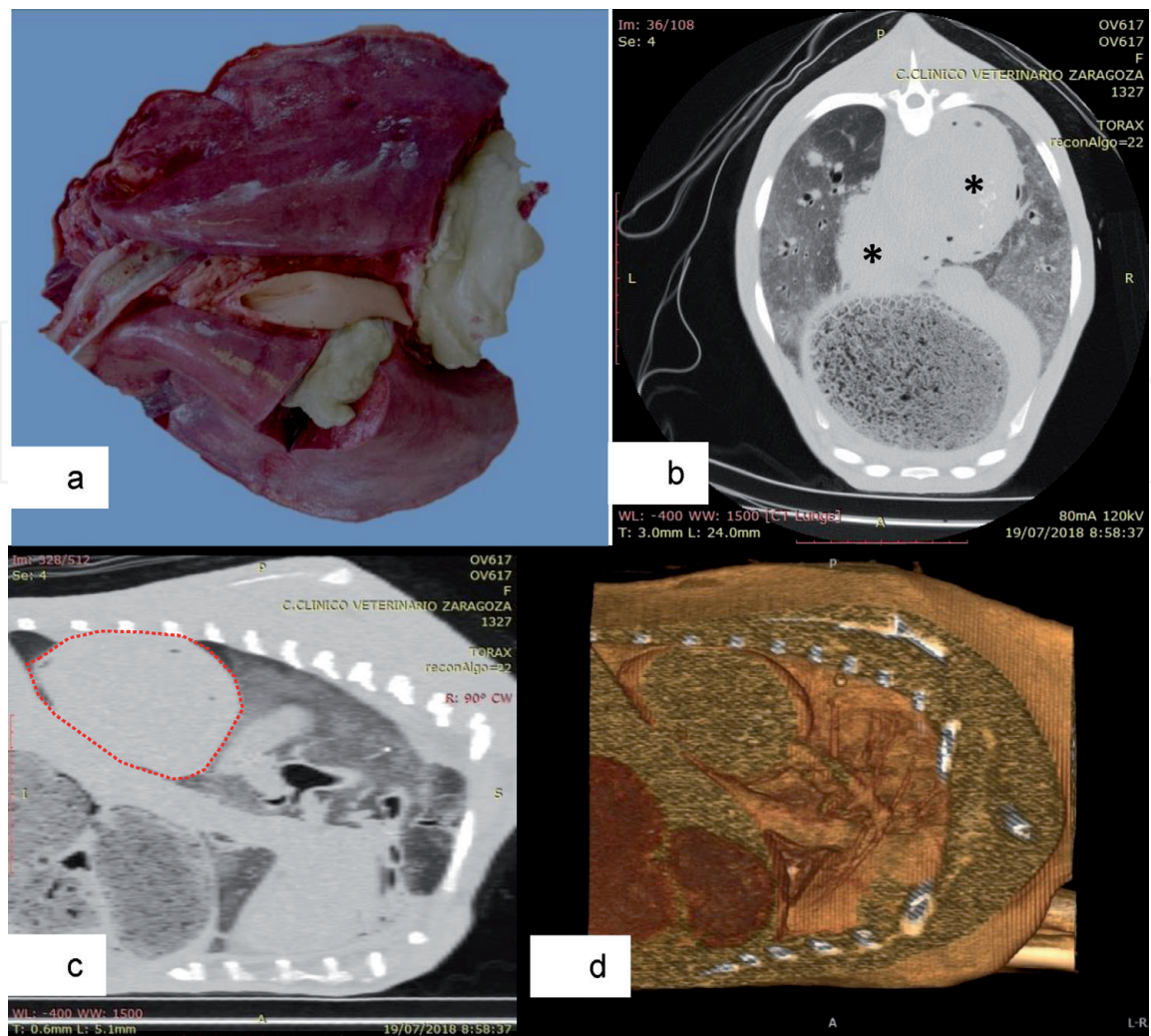


Figure 19. Lung abscess. (a) Postmortem findings with large-size abscesses in both lungs. (b) CT axial view with whitish abscesses on both sides of the mediastinum (*). (c) CT sagittal view of the right lung with a large-size abscess in caudal lobe contacting the diaphragm (red-dashed line). (d) CT 3D image where bronchial division is shown until it disappears into the abscess.

implicated [47]. Moreover, most of these bacteria exist as commensal organisms of the nasopharynx, tonsil, and lungs of healthy sheep and under certain circumstances are able to produce disease [48].

Computed tomography images reveal a good view of the injured areas. Collapsed lung areas are more opaque and whitish, while healthy tissue remains the typical gray color of a lung full of air. It is interesting to highlight that air usually remains inside the thickest bronchia even when they are surrounded by pneumonic tissue (**Figure 20a** and **b**) and that the affected tissue usually occupies the cranioventral parts of the lung (**Figure 20c** and **d**). With the computer programme associated with the CT scanner, it is possible to measure the affected area of the lung, and based on this measurement, the progression of the disease can be followed.

2.2.5 Gangrenous pneumonia (aspiration pneumonia)

Gangrenous pneumonia is a pulmonary infection commonly caused by inhalation of foreign materials, which produce inflammation and necrosis of the lung parenchyma. This is the reason why this pneumonia is also known as foreign body pneumonia, aspiration pneumonia, or necrotizing pneumonia [46, 49]. The aspirated material is usually inspired into the anteroventral lobes of the lung where it produces a moderate to severe, peracute or subacute,

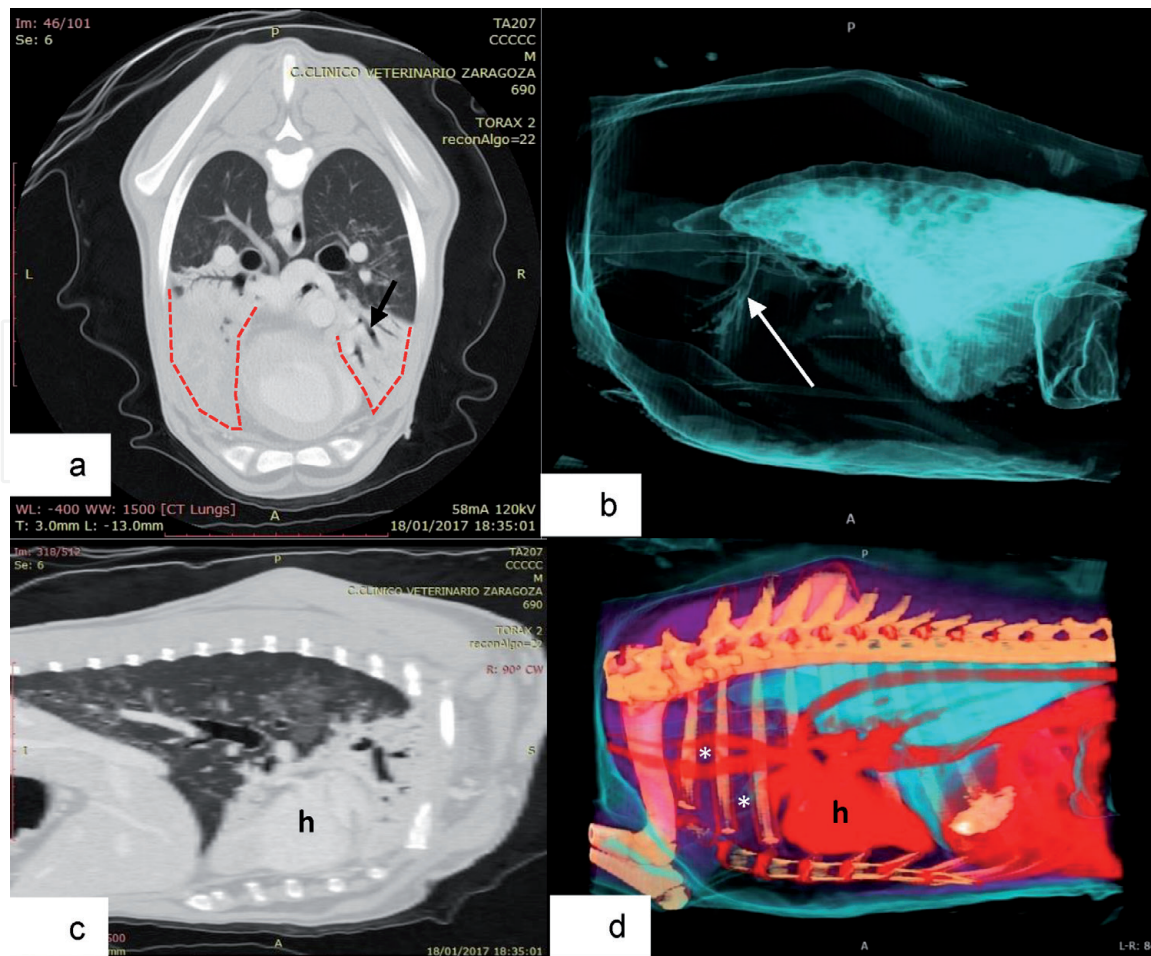


Figure 20.

Ovine respiratory complex. (a) CT axial view. Consolidation (red-dashed line) on the ventral area is appreciated, but the air remains inside the thickest bronchia (black arrow). (b) CT 3D view with airways filter. It is appreciated how the air disappears in the affected lobes, but it is kept inside the main bronchi (white arrow). (c) CT sagittal view of the right lung with iodine contrast. The peripheral area next to the heart (h) is affected and no air is found (white). (d) CT 3D image with iodine contrast and bones and skin 3 filter. It is appreciated that the air (blue) does not reach the cranioventral thoracic area (). (h): Heart in red with its vessels.*

necrotizing bronchopneumonia, depending on the composition of the inhaled material, the microorganisms involved, and the host response [46].

Aspiration of foreign material into the lung can be due to a range of causes such as rumen content during choking or when the animal is under general anesthesia, the presence of a megaesophagus, after an inappropriately oral administration of treatments, or even as a result of another respiratory disorder that hinders breathing [20, 46, 49–52].

Foreign bodies carry environmental bacteria that, when they reach the lungs, produce pulmonary necrosis foci with an accumulation of a foul-smelling exudate that sometimes could also be present in the main bronchus and trachea (**Figure 21a**), which generates a bad smell of exhaled air that is a clear clinical sign of these diseases [46].

Computed tomography images show necrotic tissue (dark or black) with diffused edges. In the injured area, necrotic content caves are present (**Figure 21b** and **c**), which can reach a large size, disappearing the lung structure as the size of the necrotic areas progresses (**Figure 21d**).

2.2.6 Pulmonary lentivirus infection

Pulmonary affection is the most severe and widespread disease form caused by small ruminant lentiviruses (SRLV) in sheep. Although lentiviral infection can

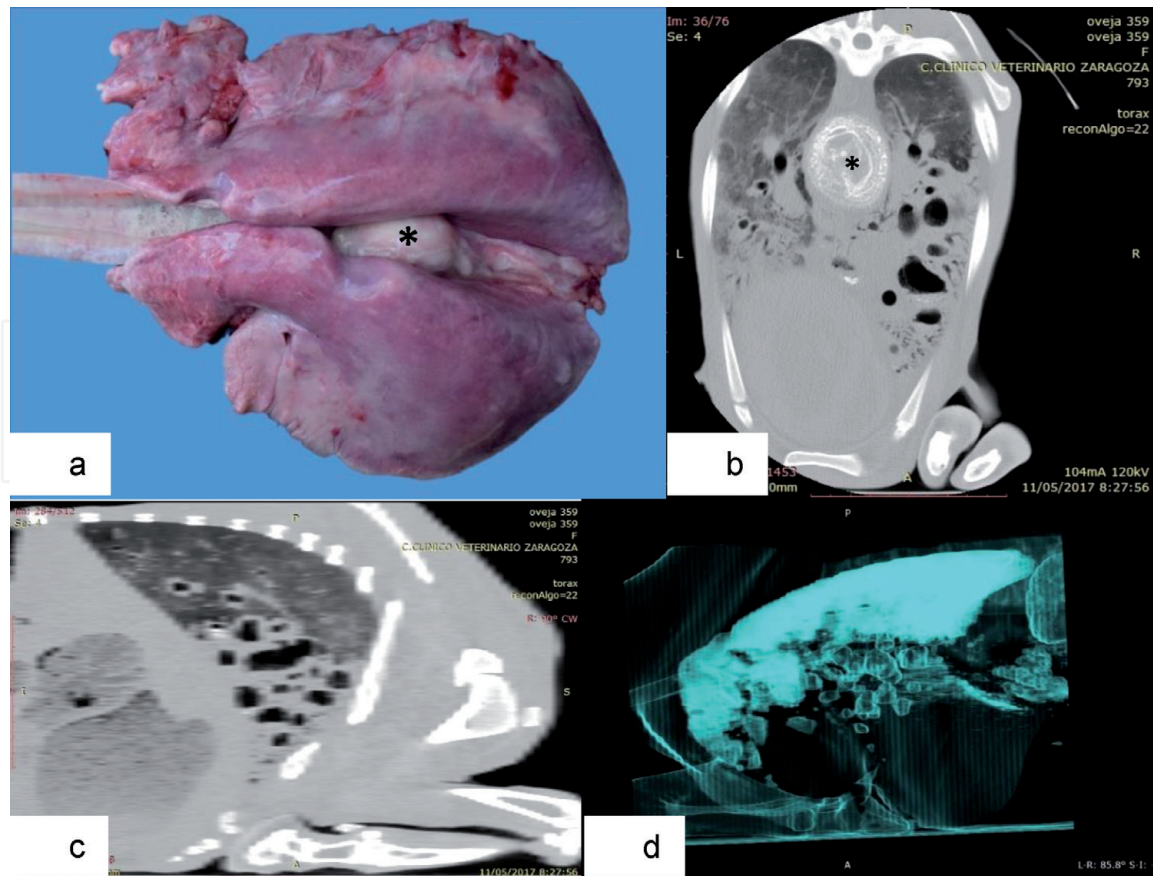


Figure 21.

Gangrenous pneumonia. (a) Pathological findings of a necrotizing bronchopneumonia and enlargement of the mediastinal lymph node (). (b) CT axial view. Cavens full of air and purulent or necrotic material, more abundant on the right lung, and typical concentric layers of caseous lymphadenitis in the mediastinal lymph node (*). (c) CT sagittal view of the right lung where the big cavens are shown. (d) CT 3D view with airways filter. Air in the dorsal area and inside the multiple cavens is appreciated, with no air in the consolidated ventral area.*

produce different clinical presentations in sheep and goats, in this article, only pulmonary lentivirus infection will be discussed.

This disease, formerly referred to as Maedi-Visna disease, is widespread in most of the countries in the world [53, 54] and generally affects adult animals. The respiratory form appears in an insidious and prolonged way, and animals show dyspnea, an increased respiratory rate, weakness, and loss of weight. If the case is uncomplicated, no cough, nasal discharge, or fever is observed. Pathological findings show an increased-size lung, both in volume and weight, and a general grayish discoloration with a myriad of gray dots in the pleural surface (**Figure 22a**). Mediastinal lymph nodes are increased in size, surpassing the limit of the diaphragmatic lobes [55].

The widespread interstitial pneumonia caused by Maedi-Visna virus (VMV) creates enormous in vivo diagnostic difficulties due to the absence of clear clinical signs and the only presence of diffuse dyspnea that can be very confusing. For this reason, imaging techniques will be very useful tools for diagnosing this disease.

Computed tomography scanner provides a detailed image of the lesion, highlighting the increased opacity in all the parenchyma associated with the interstitial pneumonia caused by VMV (**Figure 22b** and **c**). The Airways filter allows us to see a lung with little amount of air in a generalized way (**Figure 22d**).

2.2.7 Other interstitial pneumonias

Pulmonary lentivirus infection is the disease generally associated with chronic, progressive, and diffuse interstitial pneumonia, as it is confirmed by most of

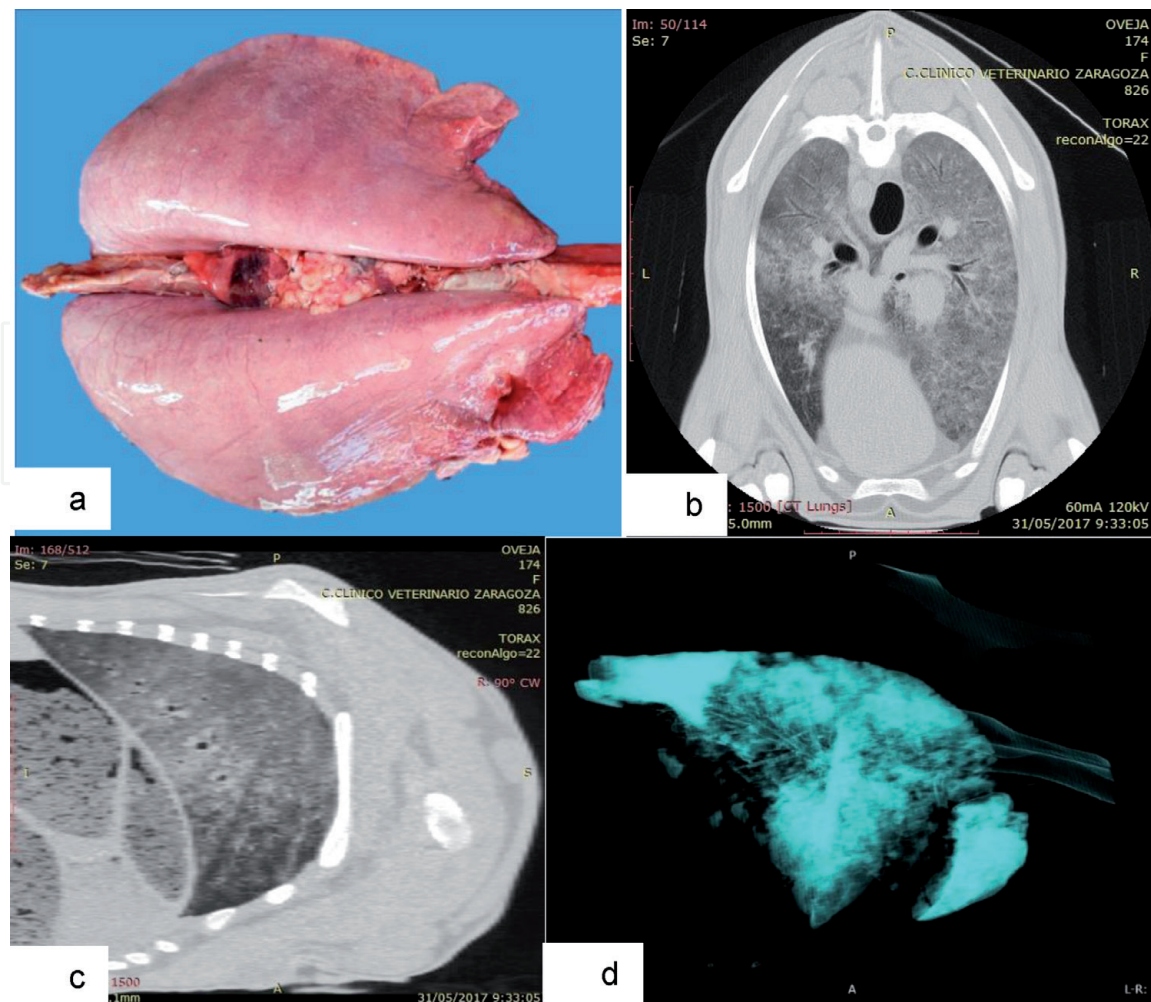


Figure 22.

Pulmonary lentivirus infection. (a) Increased-size lung with a general grayish discoloration and a myriad of gray dots in pleural surface. (b) CT axial view. Homogeneous light gray pulmonary parenchyma. (c) CT sagittal view of the right lung with the same homogeneous light gray parenchyma. (d) CT 3D view with airways filter. Less air is seen throughout the lung, except in the cranial and caudal area.

the cases found in our daily clinical work; however, there are other interstitial pneumonias affecting adult sheep, such as those caused by *Mycoplasma* sp. Although sometimes it is not possible to distinguish these two types of interstitial pneumonia macroscopically, the CT scan let us detect some cases that were not of a diffuse type but had a zonal pattern.

The clinical case presented in this section is of a zonal pattern, and, once the histopathology and microbiology was carried out, it was associated with the presence of *Mycoplasma ovipneumoniae*. Externally, the lung presented an interstitial pneumonia with a bicolor pattern, with some areas more reddened than others (**Figure 23a**).

CT scan showed lighter areas in its axial and sagittal section, located mainly in the ventral zone, and darker areas in the dorsal zone, with an intermediate area of combination of both (**Figure 23b** and **c**). CT 3D view with Airways filter showed an almost total lack of air in the dorsal area of the lung (**Figure 23d**).

2.2.8 Ovine pulmonary adenocarcinoma

Ovine pulmonary adenocarcinoma (OPA) is a contagious lung neoplasm of sheep caused by Jaagsiekte sheep retrovirus (JRSV). This disease has been reported in many of the sheep-rearing countries worldwide, being an important economic problem in the affected regions [56–58].

JSRV induces neoplastic transformation of alveolar and bronchiolar secretory epithelial cells of the distal respiratory tract, developing a tumor that can grow to occupy a significant portion of the lung [58–60].

OPA is considered as an “iceberg disease” because in OPA endemic-affected herds, the majority of animals of the flock are infected (up to 80%), but only a minority develops tumors during its productive life [58, 61, 62]. There are two pathologic forms of OPA currently recognized: classical and atypical [59].

The affected animals initially show less activity and delay in walking of the flock, followed by progressive respiratory distress, with an evidence of dyspnea and moist respiratory sounds, such as crackles and snoring, caused by the accumulation of fluid in the respiratory airways, which worsen with the increasing size of the lesions. In the final stages of the disease, variable amounts of frothy seromucous fluid are discharged from the nostrils when the sheep head is lowered [58, 59, 63]. At necropsy, neoplastic lesions are diffuse or nodular and gray or purple in color and have an increased consistency [58] (**Figure 24a**).

Computed tomography scan delivers a clear image of the primary tumor and of the satellite nodules that are generated in the metastasis phase (**Figure 24b** and **c**). Serial scanners over time allow obtaining information on the evolution of the tumor or the possible regression after its experimental treatment.

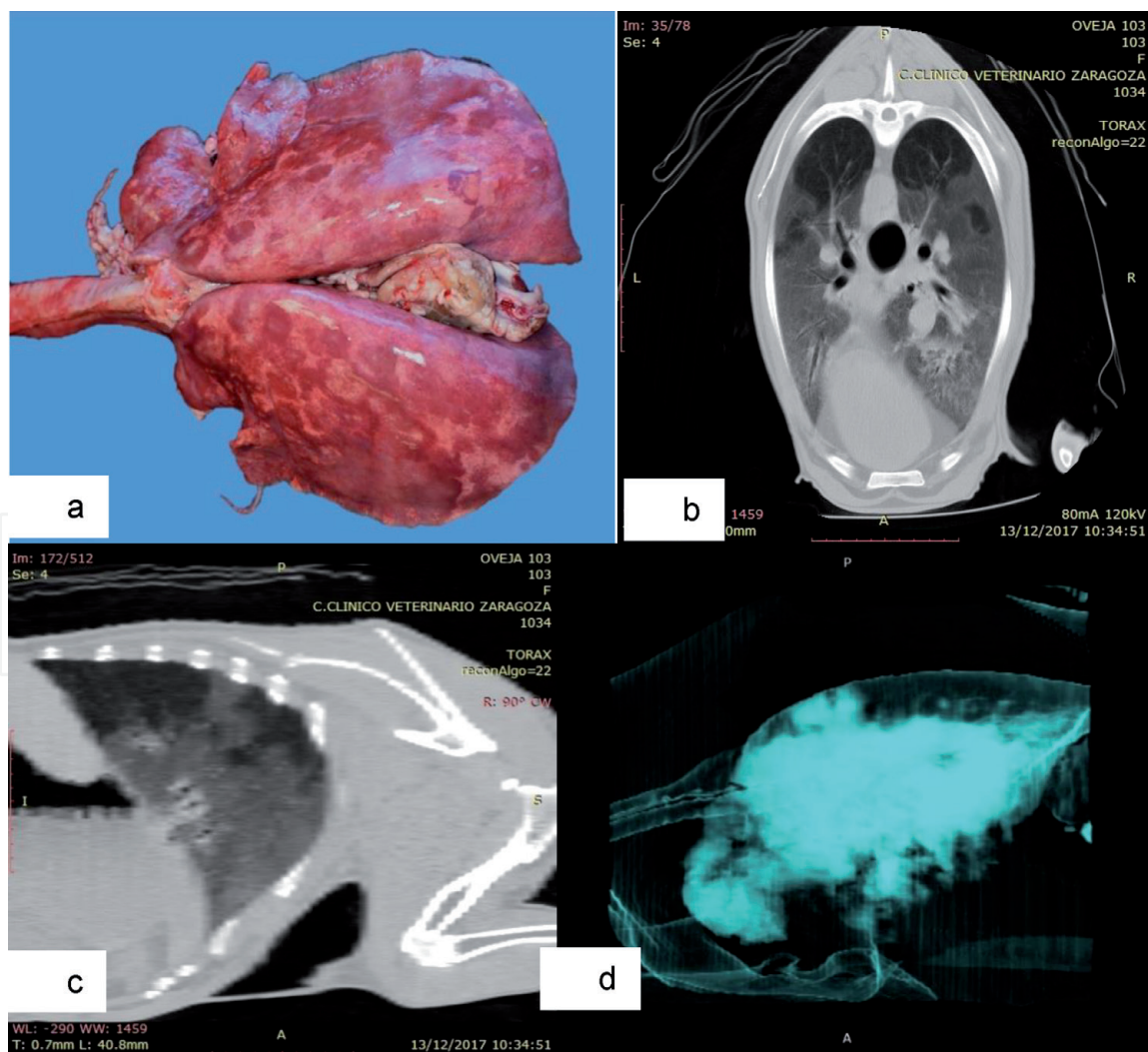


Figure 23. Interstitial pneumonia associated with *Mycoplasma sp.* (a) Increased-size bicolor nonhomogeneous lung. (b) CT axial view. Homogeneous light gray pulmonary parenchyma in the ventral area and darker in the dorsal area are observed. (c) CT sagittal view with a similar pattern to that shown in (b). (d) CT 3D view with airways filter. The completely lack of air in the dorsal area is shown.

The 3D view with Airways filter shows a total absence of air in the tumor mass and, dorsally, foci of different sizes (metastasis) also without air. These lesions are usually seen surrounded by a halo with more air than normal (**Figure 24d**).

2.2.9 Pulmonary atelectasis by compression

Lung atelectasis can occur due to compression of lung tissue, absorption of alveolar air, or impaired pulmonary surfactant production or function [64]. Atelectasis by compression is what interests us from the point of view of imaging diagnosis, because with this technology, we can diagnose the cause of compression and the place where the pressures occur.

Compression atelectasis is secondary to increased pressure exerted on the lung causing the alveoli to collapse [64], and some disorders that can cause this compression atelectasis are tumors, such as mediastinal lymphosarcomas as described in horses [65] or mediastinal thymoma as described in goats [66]. The case here presented in **Figure 25** is a large thymoma diagnosed in an adult ewe (**Figure 25a**). CT views show how the heart was displaced by the tumor to the back right side and atelectatic areas with less air near the dorsal costal wall (**Figure 25b–d**).

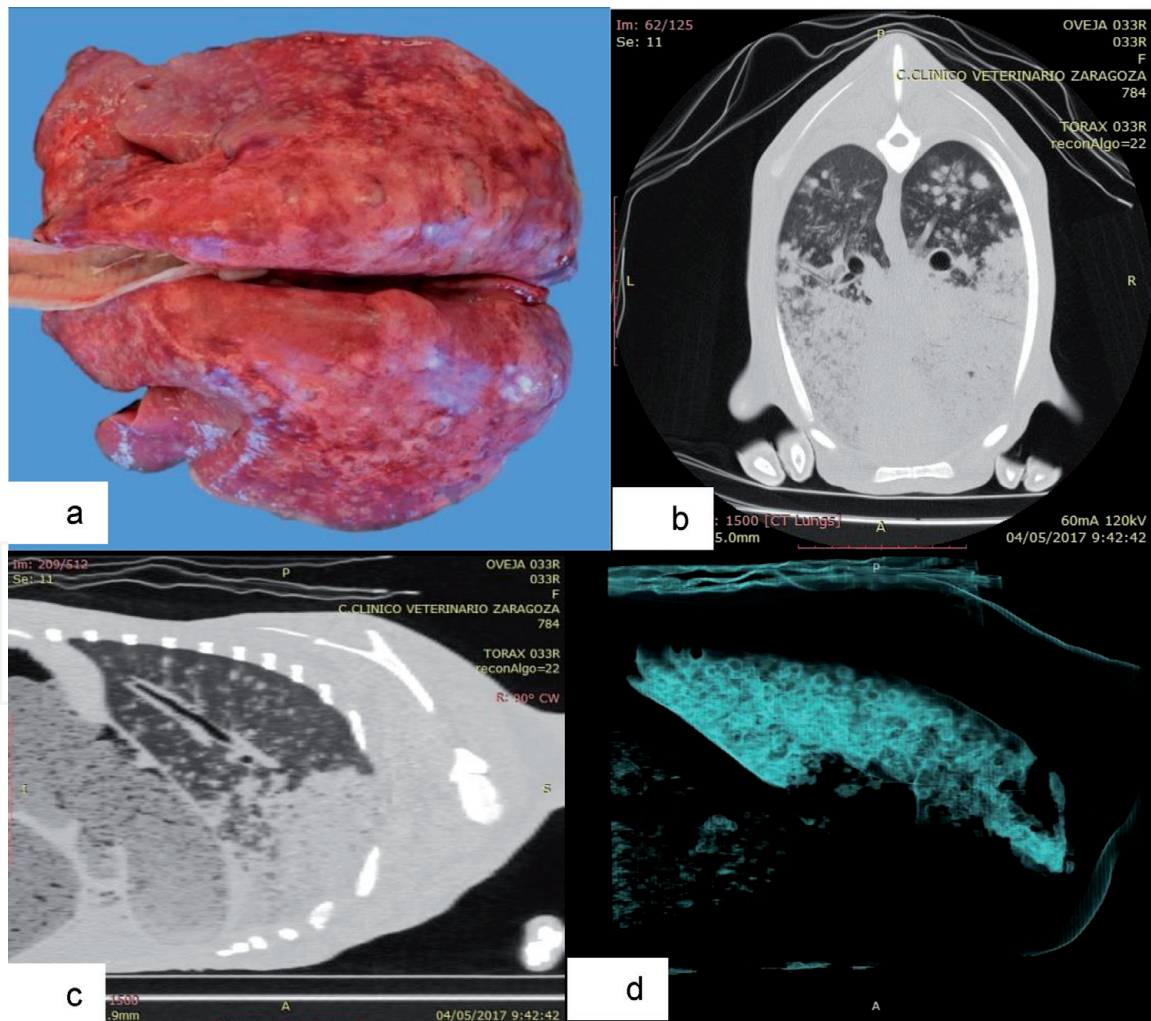


Figure 24. Ovine pulmonary adenocarcinoma. (a) Grayish cranioventral areas and satellite nodules of the tumor. (b) CT axial view. Grayish pulmonary parenchyma with white spots (metastasis) in the dorsal area and homogeneous clear white in the ventral area (main tumor) are shown. (c) CT sagittal view of the same lung with the same pattern as (b). (d) CT 3D view with airways filter. Air is appreciated in the back-caudal area, decreasing towards cranial and disappearing into the cranioventral area where main tumor mass is located. Multiple air rings can be seen surrounding the foci of metastasis.

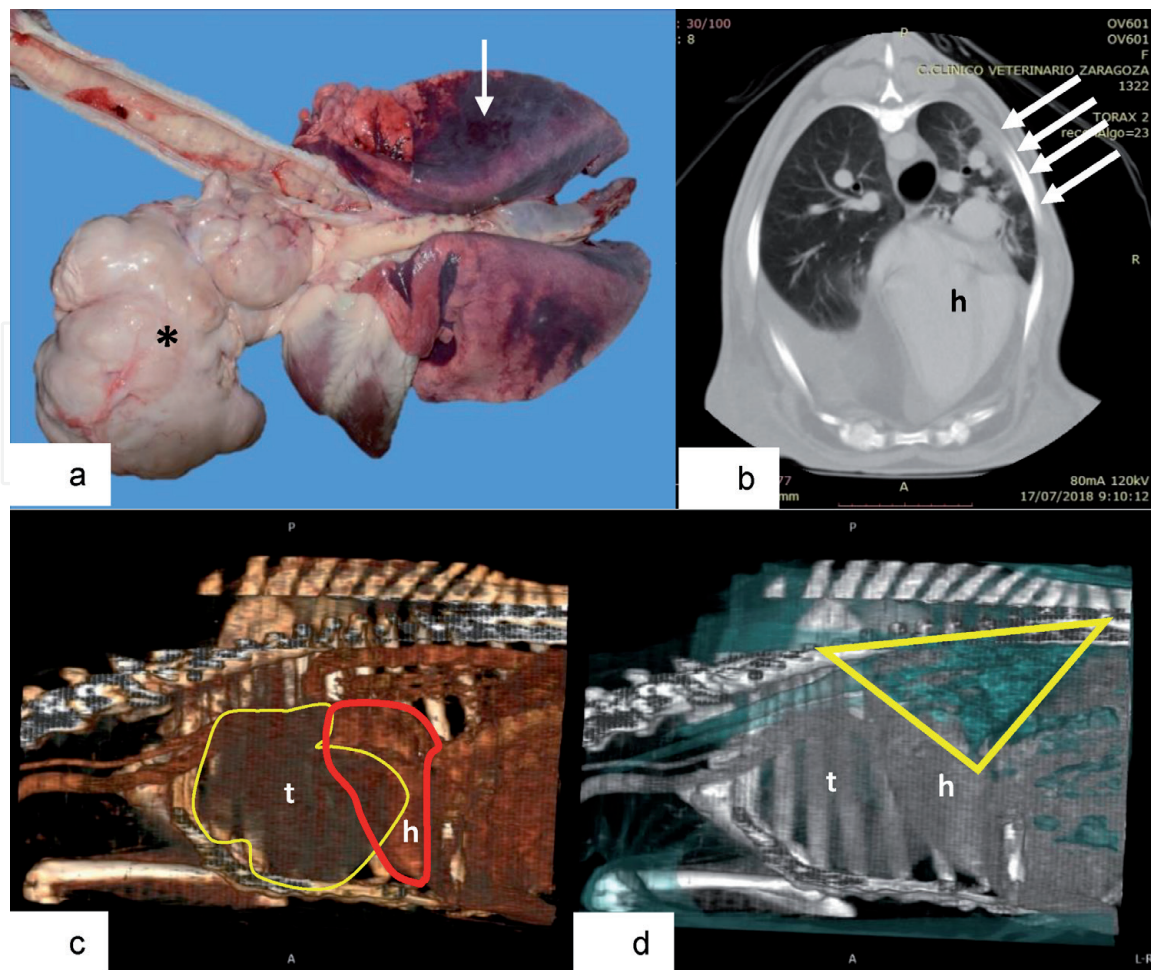


Figure 25. Compression atelectasis. (a) Large-size thymoma (*) causing lung atelectasis, especially in the right side (white arrow). (b) CT axial view. The heart has been displaced by the tumor to the back right side (h). Near the costal wall, atelectatic areas with less air can be seen (white arrows). (c) CT 3D sagittal view, right side. Thymoma (t and yellow line) and heart (h and red line) are shown. (d) CT 3D view with bones and skin 2 filter. Air is appreciated in the back-caudal area, behind the heart (yellow triangle).

Likewise, abscesses or pyogranulomas located in mediastinal lymph nodes or thoracic cavity, such as those of caseous lymphadenitis (CLA) caused by *Corynebacterium pseudotuberculosis*, can produce severe compression atelectasis (Figure 26a and b). The visceral form of CLA commonly causes lesions in the mediastinal lymph nodes and lung parenchyma, producing severe respiratory clinical signs [67]. In a study carried out in our service on 123 culled sheep, 32% of the animals had CLA lesions, of which 70% had the visceral form of the disease, with 80.9% having lesions in the thoracic cavity [46]. In Figure 26c and d, CT 3D views show the location and size of the affected lymph nodes and a small area of atelectasis without air. Lastly, compression atelectasis can be also caused by pleural abscesses, diaphragmatic hernias, megaesophagus, or even prolonged decubitus [51, 68].

CT scan is a very suitable tool to find the cause, the situation, and the size of compression; however, it is difficult to visualize the thin layer of atelectatic tissue that can be produced next to the pressing mass or in the projection on the rib area.

3. Conclusions

The health of a flock is based on a proper diagnosis of the main disorders that affect the farm. Imaging tools have improved the diagnostic process and are essential today.

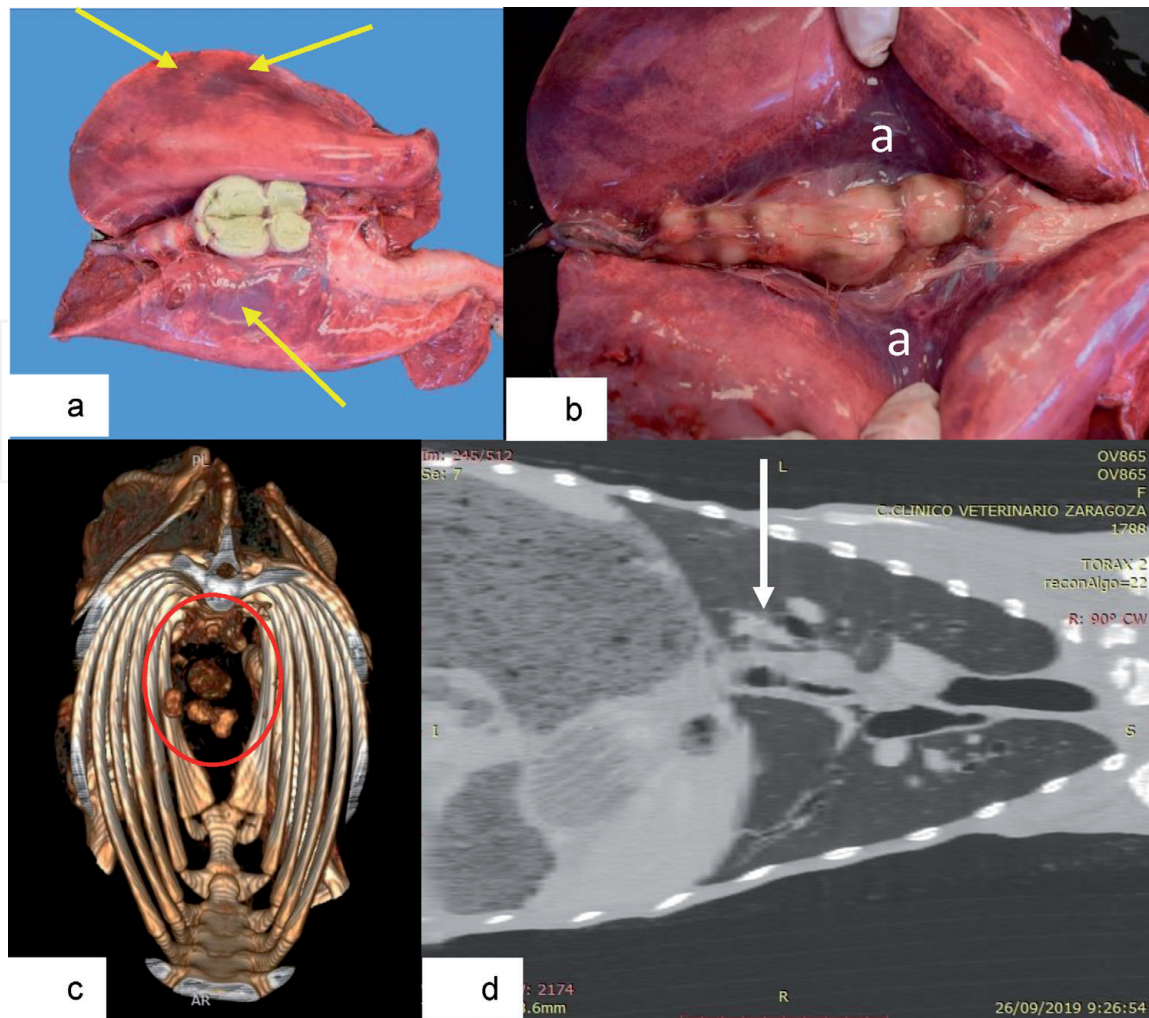


Figure 26.

Compression atelectasis. (a) Caseous lymphadenitis affecting mediastinal lymph node causing lung atelectasis in mediastinal and costal side (yellow arrows). (b) Lung atelectasis (a) in contact area with affected lymph nodes. (c) CT 3D view where the location and size of the affected lymph nodes can be seen (red circle). (d) CT coronal view, where it highlighted (white arrow) a small area of atelectasis without air.

Thermography has become a useful and inexpensive tool for approaching the diagnosis of upper respiratory tract diseases. However, the use of computed tomography is more expensive and specific, reserving for the detection of important herd problems that justify its expense. It is also necessary in the investigation and monitoring of processes or treatments that have not been proven. This tool helps in an interesting way to understand the pathogenesis and lesional location since we can study the different structures and the interrelation between them in the original position.

The diagnosis of respiratory disorders in ruminants has evolved significantly thanks to the application of different imaging diagnostic techniques, detecting some diseases that until recently were little known.

Acknowledgements

We would like to thank the collaboration of veterinarians and farmers who send their interesting clinical cases to the Ruminant Clinical Service of the Veterinary Hospital (SCRUM). In addition, we would like to acknowledge the use of Servicio General de Apoyo a la Investigación-SAI, Universidad de Zaragoza.

This study was supported by the Aragón Government and the European Social Fund (Construyendo Aragón 2016–2020).

Conflict of interest

The authors have nothing to disclose.

IntechOpen

Author details

Luis Miguel Ferrer^{1*}, Juan José Ramos¹, Enrique Castells², Héctor Ruíz¹,
María Climent¹ and Delia Lacasta¹

1 Animal Pathology Department, Instituto Agroalimentario de Aragón-IA2
(Universidad de Zaragoza-CITA), Veterinary Faculty of Zaragoza, Zaragoza, Spain

2 Centro Clínico Veterinario, Zaragoza, Spain

*Address all correspondence to: lmferrer@unizar.es

IntechOpen

© 2020 The Author(s). Licensee IntechOpen. This chapter is distributed under the terms of the Creative Commons Attribution License (<http://creativecommons.org/licenses/by/3.0>), which permits unrestricted use, distribution, and reproduction in any medium, provided the original work is properly cited. 

References

- [1] Frandson RD, Wilke WL, Fails AD. Anatomy and Physiology of Farm Animals. 7th ed. Nueva Jersey, Estados Unidos: Wiley-Blackwell; 2009. ISBN-13: 978-0-8138-1394-3
- [2] Redaelli V, Caglio S. Thermal imaging theory. In: Luzi F, Mitchell M, Costa LN, Redaelli V, editors. Thermography: Current Status and Advances in Livestock Animals and in Veterinary. Brescia, Italy: Fondazione Iniziative Zooprofilattiche e Zootecniche; 2013. pp. 41-46. ISBN: 978-8-8975-6206-1
- [3] Meehan JT, Brogden KA, Courtney C, Cutlip RC, Lehmkuhl HD. Chronic proliferative rhinitis associated with *Salmonella arizonae* in sheep. *Veterinary Pathology*. 1992;**29**:556-559. DOI: 10.1177/030098589202900616
- [4] Lacasta D, Ferrer LM, Ramos JJ, Bueso JP, Borobia M, de Arcaute MR, et al. Chronic proliferative rhinitis associated with *Salmonella enterica* subspecies diarizonae serovar 61: k: 1, 5, (7) in sheep in Spain. *Journal of Comparative Pathology*. 2012;**147**:406-409. DOI: 10.1016/j.jcpa.2012.03.004
- [5] Rubira I, Figueras L, De las Heras M, Bueso JP, Castells E, Climent M, et al. Chronic proliferative rhinitis in sheep: An update. *Small Ruminant Research*. 2019;**179**:21-25. DOI: 10.1016/j.smallrumres.2019.09.001
- [6] Wolf C, Schefers J. Challenges posed by a flock problem of *Salmonella* diarizonae induced proliferative rhinitis. In: Proceedings of the 9th International Sheep Veterinary Congress; 22-26 May 2017; Harrogate, United Kingdom
- [7] Stokar-Regenscheit N, Overesch G, Giezendanner R, Roos S, Gurtner C. *Salmonella enterica* subsp. diarizonae serotype 61:k:1,5, (7) associated with chronic proliferative rhinitis and high nasal colonization rates in a flock of Texel sheep in Switzerland. *Preventive Veterinary Medicine*. 2017;**145**:78-82. DOI: 10.1016/j.prevetmed.2017.07.003
- [8] López-Tamayo S, Rubira I, De las Heras M, Castells E, Lacasta D. Use of thermography for the diagnosis of chronic proliferative rhinitis in sheep and its application in the differential diagnosis of the first case affecting the dorsal turbinate. *Veterinary Record Case Report*. 2020;**8**:e001070. DOI: 10.1136/vetreccr-2020-001070
- [9] De las Heras M, Ortín A, Borobia M, Navarro T. Enzootic nasal adenocarcinoma in sheep: An update. *Small Ruminant Research*. 2019;**180**:131-134. DOI: 10.1007/978-3-642-55638-8_8
- [10] Ortín A, Cousens C, Minguijon E, Pascual Z, de Villarreal MP, Sharp JM, et al. Characterization of enzootic nasal tumour virus of goats: Complete sequence and tissue distribution. *The Journal of General Virology*. 2003;**84**:2245-2252. DOI: 10.1099/vir.0.19125-0
- [11] McKinnon AO, Thorsen J, Hayes MA, Misener CR. Enzootic nasal adenocarcinoma of sheep in Canada. *The Canadian Veterinary Journal*. 1982;**23**(3):88-94
- [12] De las Heras M, Ortín A, Cousens C, Minguijón E, Sharp JM. Enzootic nasal adenocarcinoma of sheep and goats. In: Fan H, editor. Jaagsiekte Sheep Retrovirus and Lung Cancer. Current Topics in Microbiology and Immunology. Vol. 275. Berlin, Heidelberg: Springer; 2003. ISBN: 978-3-642-62897-9. DOI: 10.1007/978-3-642-55638-8_8
- [13] Švara T, Gombač M, Vrecl M, Juntos P, Pogačnik M. Enzootic nasal adenocarcinoma of sheep. *Slovenian Veterinary Research*. 2006;**43**(2):71-75. UDC 619:626.211-006-07:636.3

- [14] Gunalan S, Kamaliah G, Wan S, Rozita AR, Rugayah M, Osman MA, et al. Sheep oestrosis (*Oestrus ovis*, Diptera: Oestridae) in Damara crossbred sheep. *Malaysian Journal of Veterinary Research*. 2011;**2**:41-49
- [15] Gracia MJ, de Arcaute MR, Ferrer LM, Ramo M, Jiménez C, Figueras L. Oestrosis: Parasitism by *Oestrus ovis*. *Small Ruminant Research*. 2019;**181**:91-98. DOI: 10.1016/j.smallrumres.2019.04.017
- [16] Gracia MJ, Lucientes J, Peribáñez MA, Castillo JA, Calvete C, Ferrer LM. Epidemiology of *Oestrus ovis* infection of sheep in Northeast Spain (mid-Ebro Valley). *Tropical Animal Health and Production*. 2010;**42**(5):811-813. DOI: 10.1007/s11250-009-9503-8
- [17] Özdal N, Tanritanir P, Ilhan F, Değer S. The prevalence of ovine oestrosis (*Oestrus ovis* Linnaeus, 1761, Diptera: Oestridae) and risk factors in eastern Turkey. *Veterinarski Arhiv*. 2016;**86**(3):323-333
- [18] Alem F, Kumsa B, Degefu H. *Oestrus ovis* larval myiasis among sheep and goats in Central Oromia, Ethiopia. *Tropical Animal Health and Production*. 2010;**42**(4):697-703. DOI: 10.1007/s11250-009-9477-6
- [19] Gebremedhin EZ. Prevalence of ovine and caprine oestrosis in ambo, Ethiopia. *Tropical Animal Health and Production*. 2011;**43**(1):265-270. DOI: 10.1007/s11250-010-9687-y
- [20] Ferrer LM, Garcia de Jalon JA, De las Heras M. *Atlas de Patología Ovina*. Zaragoza, Spain: Servet Diseño y Comunicación S.L.; 2009. p. 312. ISBN-10: 8493292117
- [21] Benavides J, González L, Dagleish M, Pérez V. Diagnostic pathology in microbial diseases of sheep or goats. *Veterinary Microbiology*. 2015;**181**:15-26. DOI: 10.1016/j.vetmic.2015.07.012
- [22] Castells E, Lacasta D, Climent M, Pérez M, Sanromán F, Jiménez C, et al. Diagnostic imaging techniques of the respiratory tract of sheep. *Small Ruminant Research*. 2019;**180**:112-126. DOI: 10.1016/j.smallrumres.2019.05.021
- [23] Freeman DE. Sinus disease. *Veterinary Clinics: Equine Practice*. 2003;**19**(1):209-243. DOI: 10.1016/S0749-0739(02)00062-7
- [24] Jesse FA, Abba Y, Sadiq MA, Umer M, Chung ELT, Bitrus AA, et al. A suspected case of suppurative frontal sinusitis in a Friesian heifer: Clinical management. *International Journal of Livestock Research*. 2016;**6**(8):50-54. DOI: 10.5455/ijlr.20160816055652
- [25] Kumar PR, Prasad VD, Sreenu M, Raju DB. Surgical management of frontal sinusitis in a buffalo. *Research & Reviews: Journal of Veterinary Science and Technology*. 2018;**6**(1):3-5. DOI: 10.37591/rrjovst.v6i1.553
- [26] Mehra P, Jeong D. Maxillary sinusitis of odontogenic origin. *Current Allergy and Asthma Reports*. 2009;**9**(3):238-243. DOI: 10.1007/s11882-009-0035-0
- [27] Schild CO, Caffarena RD, Rabaza A, Banchemo G, Giannitti F, Dantas AF, Maia LA, Riet F. Nasal conidiobolomycosis in a sheep (*Ovis aries*) in Uruguay. *Veterinaria (Montevideo)*. 2016;**52**(203):4
- [28] Daniela M. The prevalence of wormy sinusitis in goats from the west side of our country. *Scientific Papers Animal Science and Biotechnologies*. 2008;**41**(2):762-764
- [29] Gergeleit H, Bienert-Zeit A, Ohnesorge B. Cytologic and microbiological examination of secretions from the paranasal sinuses in horses and other species. *Journal of Equine Veterinary Science*. 2018;**61**:22-31. DOI: 10.1016/j.jevs.2017.11.001

- [30] Sáez T, Ramos JJ, García de Jalón JA, Unzueta A, Loste A. Laryngeal hemiplegia in a ram associated with *Sarcocystis* species infection. *The Veterinary Record*. 2003;**153**(1):27-28. DOI: 10.1136/vr.153.1.27
- [31] Edmunds JL, Mcwan MN. Factors affecting the development of laryngeal chondritis in sheep. *Large Animal Review*. 2017;**23**(6):219-222. Held on OpenAIR [online]. Available from: <https://openair.rgu.ac.uk>
- [32] Climent S, Sarasa M, Muniesa P, Latorre R, Terrado J, Climent M. Embriología y anatomía veterinaria Vol.2: Cabeza, aparatos respiratorio, digestivo y urogenital. SNC y órganos de los sentidos. Zaragoza: Acribia; 2012. ISBN: 978-84-200-1166-0
- [33] Kim KJ, Critz AM, Crandall ED. Transport of water and solutes across sheep visceral pleura. *The American Review of Respiratory Disease*. 1979;**120**:883-892. DOI: 10.1164/arrd.1979.120.4.883
- [34] Lacasta D, González JM, Navarro T, Saura F, Acín C, Vasileiou NGC. Significance of respiratory diseases in the health management of sheep. *Small Ruminant Research*. 2019;**181**:99-102. DOI: 10.1016/j.smallrumres.2019.03.004
- [35] Ortega M, González JM, Ramos JJ, Ferrer LM, Ruiz de Arcaute M, Lacasta D, et al. Estudio de las alteraciones de la tráquea en el ganado ovino: Descripción y prevalencia. In: XLII Congreso Nacional y XVIII Congreso Internacional de la Sociedad Española de Ovinotecnia y Caprinotecnia, 20-22 September 2017; Salamanca, Spain. 2017. pp. 373-378
- [36] María GA, Miranda de la Lama G. Ovinotecnia: Producción y economía de la especie ovina. In: Aspectos de bienestar animal en la especie ovina. Zaragoza: Prensas Universitarias de Zaragoza; 2009. pp. 57-64. ISBN: 978-84-92521-89-0
- [37] Tena L, Ortega M, Jiménez JC, Forcano D, Menjón A, Lacasta D, et al. Estudio de la relación entre el aplastamiento traqueal y las patologías pulmonares en ganado ovino adulto. In: XLIV Congreso Nacional y XX Congreso Internacional de la Sociedad Española de Ovinotecnia y Caprinotecnia; 18-20 Septiembre 2019; Córdoba, Spain. 2019. pp. 459-463
- [38] Deplazes P, Eckert J, Mathis A, von Samson-Himmelstjerna G, Zahner H. Parasitology in Veterinary Medicine. The Netherlands: Wageningen Academic Publishers; 2016. p. 653. DOI: 10.3920/978-90-8686-274-0
- [39] Panayotova-Pencheva MS, Alexandrov MT. Some pathological features of lungs from domestic and wild ruminants with single and mixed protostrongylid infections. *Veterinary Medicine International*. 2010;**74**:1062-9. DOI: 10.4061/2010/741062
- [40] Al-Anbagi NA. Isolation and identification some bacterial causes of lung abscesses sheep by chromogenic media. *Basrah Journal of Veterinary Research*. 2016;**15**(2):360-370. DOI: 10.33762/bvetr.2016.124337
- [41] Yegoraw AA, Gebremeskel AK, Tesema TS, Birhanu BT. Aerobic and anaerobic bacterial isolates from the respiratory tract of sheep slaughtered at Addis Ababa Abattoirs Enterprises, Central Ethiopia. *Journal Veterinary Medicine Animal Health*. 2017;**10**:284-289. DOI: 10.5897/JVMAH2017.0574
- [42] Bell S. Respiratory disease in sheep: 1. Differential diagnosis and epidemiology. In *Practice*. 2008;**30**(4):200-207
- [43] Singer AJ, Talan DA. Management of skin abscesses in the era of methicillin-resistant *Staphylococcus aureus*. *New England Journal of Medicine*. 2014;**370**(11):1039-1047. DOI: 10.1056/NEJMra1212788

- [44] de la Fuente R, de las Heras M, Torrijos C, Diez de Tejada P, Pérez-Sancho M, Carrión FJ, et al. Short communication: Isolation frequency of bacteria causing lymphadenitis and abscesses in small ruminants in Central Spain. *Small Ruminant Research*. 2017;**154**:5-8. DOI: 10.1016/j.smallrumres.2017.06.022
- [45] Abass KS, Mohammed NS, Taleb M, Raheem ZS. Study of bovine and ovine pulmonary and hepatic abscessation at Kirkuk abattoir. *Plant Archives*. 2019;**19**(2):1640-1644
- [46] Lacasta D, Fernández A, González JM, Ramos JJ, Ortín A, Ferrer LM. Gangrenous pneumonia, ovine respiratory complex and visceral form of caseous lymphadenitis: Relevance in lower respiratory tract disorders of adult sheep. *Small Ruminant Research*. 2019;**180**:100-105. DOI: 10.1016/j.smallrumres.2019.08.004
- [47] Miller DS, Weiser GC, Ward ACS, Drew ML, Chapman PL. Domestic sheep (*Ovis aries*) Pasteurellaceae isolates from diagnostic submissions to the Caine veterinary teaching center (1990-2004). *Veterinary Microbiology*. 2011;**150**:284-288. DOI: 10.1016/j.vetmic.2011.01.024
- [48] Glendinning L, Wright S, Pollock J, Tennant P, Collie D, McLachlan G. Exploring the variability of the sheep lung microbiota. *Applied and Environmental Microbiology*. 2016;**82**:3225-3238. DOI: 10.1128/AEM.00540-16
- [49] Scott PR. Overview of Aspiration Pneumonia. *MSD Veterinary Manual* [Internet]. 2017. Available from: <https://www.msddvetmanual.com/respiratory-system/aspiration-pneumonia/overview-of-aspiration-pneumonia> [Accessed: 28 January 2020]
- [50] Blowey R, Weaver AD. *Color Atlas of Diseases and Disorders of Cattle*. E-Book. 3rd ed. Mosby Ltd: Elsevier Health Sciences; 2011. p. 280. ISBN: 9780723436867
- [51] do Prado Guirro ECB, Martin CC, Hilgert AR, Pagliosa GM, Silva MM. Clinical, radiographic and pathological analyses of megaesophagus in sheep – Case report. *Revista Veterinária em Foco*. 2017;**15**(1):54-58
- [52] Darcy HP, Humm K, ter Haar G. Retrospective analysis of incidence, clinical features, potential risk factors, and prognostic indicators for aspiration pneumonia in three brachycephalic dog breeds. *Journal of the American Veterinary Medical Association*. 2018;**253**(7):869-876. DOI: 10.2460/javma.253.7.869
- [53] Christodoulopoulos G. Maedi–Visna: Clinical review and short reference on the disease status in Mediterranean countries. *Small Ruminant Research*. 2006;**62**(1-2):47-53. DOI: 10.1016/j.smallrumres.2005.07.046
- [54] Minguijón E, Reina R, Pérez M, Polledo L, Villoria M, Ramírez H, et al. Small ruminant lentivirus infections and diseases. *Veterinary Microbiology*. 2015;**181**(1-2):75-89. DOI: 10.1016/j.vetmic.2015.08.007
- [55] Luján L, Pérez M, de Andrés D, Reina R. Pulmonary lentivirus infection in sheep. *Small Ruminant Research*. 2019;**181**:87-90. DOI: 10.1016/j.smallrumres.2019.05.006
- [56] Cousens C, Thonur L, Imlach S, Crawford J, Sales J, Griffiths DJ. Jaagsiekte sheep retrovirus is present at high concentration in lung fluid produced by ovine pulmonary adenocarcinoma-affected sheep and can survive for several weeks at ambient temperatures. *Research in Veterinary Science*. 2009;**87**(1):154-156. DOI: 10.1016/j.rvsc.2008.11.007
- [57] Sonawane GG, Tripathi BN, Kumar R, Kumar J. Diagnosis and

- prevalence of ovine pulmonary adenocarcinoma in lung tissues of naturally infected farm sheep. *Veterinary World*. 2016;**9**(4):365-370. DOI: 10.14202/vetworld.2016.365-370
- [58] Ortín A, De las Heras M, Borobia M, Ramo MA, Ortega M, Ruiz de Arcaute M. Ovine pulmonary adenocarcinoma: A transmissible lung cancer of sheep, difficult to control. *Small Ruminant Research*. 2019;**176**:37-41. DOI: 10.1016/j.smallrumres.2019.05.014
- [59] De las Heras M, González L, Sharp JM. Pathology of ovine pulmonary adenocarcinoma. In: *Jaagsiekte Sheep Retrovirus and Lung Cancer*. Berlin Heidelberg: Springer-Verlag; 2003. pp. 25-54. DOI: 10.1007/978-3-642-55638-8
- [60] Griffiths DJ, Martineau HM, Cousens C. Pathology and pathogenesis of ovine pulmonary adenocarcinoma. *Journal of Comparative Pathology*. 2010;**142**(4):260-283. DOI: 10.1016/j.jcpa.2009.12.013
- [61] Caporale M, Centorame P, Giovannini A, Sacchini F, Di Ventura M, De las Heras M, et al. Infection of lung epithelial cells and induction of pulmonary adenocarcinoma is not the most common outcome of naturally occurring JSRV infection during the commercial lifespan of sheep. *Virology*. 2005;**338**(1):144-153. DOI: 10.1016/j.virol.2005.05.018
- [62] Benito A. Estudio Sobre la Infección y Transmisión del Retrovirus Ovino de Jaagsiekte en un Rebaño Ovino Afectado de Adenocarcinoma Pulmonar Ovino [thesis]. Zaragoza, Spain: University of Zaragoza; 2010
- [63] Palmarini M, Fan H. Retrovirus-induced ovine pulmonary adenocarcinoma, an animal model for lung cancer. *Journal of the National Cancer Institute*. 2001;**93**(21):1603-1614. DOI: 10.1093/jnci/93.21.1603
- [64] Grott K, Dunlap JD. Atelectasis. *StatPearls* [Internet]. 2019. Available from: <https://www.ncbi.nlm.nih.gov/books/NBK545316/> [Accessed: 20 January 2020]
- [65] De Clercq D, van Loon G, Lefère L, Deprez P. Ultrasound-guided biopsy as a diagnostic aid in three horses with a cranial mediastinal lymphosarcoma. *The Veterinary Record*. 2004;**154**(23):722-726. DOI: 10.1136/vr.154.23.722
- [66] Braun U, Warislohner S, Gerspach C, Ohlerth S, Wanninger S, Borel N. Clinical, sonographic and pathological findings in a Saanen goat with mediastinal thymoma. *Schweizer Archiv für Tierheilkunde*. 2017;**159**(3):185-188. DOI: 10.17236/sat00111
- [67] Windsor PA. Control of caseous lymphadenitis. *The Veterinary Clinics of North America. Food Animal Practice*. 2011;**27**:93-202. DOI: 10.1016/j.cvfa.2010.10.019
- [68] Scott PR, Sargison ND. Ultrasonography as an adjunct to clinical examination in sheep. *Small Ruminant Research*. 2010;**92**(1-3):108-119. DOI: 10.1016/j.smallrumres.2016.12.021